UNIVERSIDADE FEDERAL DE CIÊNCIAS DA SAÚDE DE PORTO ALEGRE

PROGRAMA DE PÓS-GRADUAÇÃO EM CIÊNCIAS DA SAÚDE

Roger Kist

Estudos estruturais do complexo enzimático mTOR (*mechanistic target of rapamycin*) com abordagem *in silico* para delineamento de estratégias para desenvolvimento racional de inibidores do complexo enzimático

Porto Alegre

2022

Roger Kist

Estudos estruturais do complexo enzimático mTOR (*mechanistic target of rapamycin*) com abordagem *in silico* para delineamento de estratégias para desenvolvimento racional de inibidores do complexo enzimático

Tese submetida ao Programa de Pós-Graduação em Ciências da Saúde da Universidade Federal de Ciências da Saúde de Porto Alegre como requisito para a obtenção do grau de Doutor.

Orientador: Prof. Dr. Rafael Andrade Caceres

Porto Alegre
2022

Catalogação na Publicação

Kist, Roger
Estudos estruturais do complexo enzimático mTOR (mechanistic target of rapamycin) com abordagem in silico para delineamento de estratégias para desenvolvimento racional de inibidores do complexo enzimático / Roger Kist. -- 2022.
80 p. : il., graf., tab. ; 30 cm.

Tese (doutorado) -- Universidade Federal de Ciências da Saúde de Porto Alegre, Programa de Pós-Graduação em Ciências da Saúde, 2022.

Orientador(a): Rafael Andrade Caceres.

1. mTOR. 2. mLst8. 3. Modelos coarse-grained. 4. Dinâmica molecular. 5. Interação proteína-proteína. I. Título.

Sistema de Geração de Ficha Catalográfica da UFCSPA com os dados fornecidos pelo(a) autor(a).

Dedico este trabalho a todos que tornaram esta façanha realidade.

AGRADECIMENTOS

Aos meus pais, Nedi e Renato, meus formadores de caráter e sempre incansáveis para que eu atingisse êxito nos meus estudos.

À minha namorada, Natália, pelo companheirismo e por acreditar na nossa superação de desafios.

Ao amigo e professor Rafael, por toda a confiança depositada em mim desde a graduação, pela excelente orientação cedida durante o desenvolvimento do trabalho e pela autonomia que sempre possibilitou a mim.

Ao Luís pela imensa colaboração efetuada no trabalho e pelas discussões de estratégias aplicadas nos estudos efetuados.

Aos colegas da Santa Casa – onde descobri meu alvo de trabalho – pela parceria e auxílio nesta dupla jornada.

Aos colegas e alunos com os quais pude compartilhar conhecimentos e auxiliá-los nos seus trabalhos.

Enfim, muito obrigado a todos que contribuíram de alguma forma para esta conquista.

“I have always prided myself that I do my own thinking. I have my own philosophy. I have my own answer to the reasons things have turned out in my life.”

Cmd Major Richard Davis Winters
E Co., 2nd Bn., 506th PIR, 101st AD

RESUMO

A via PI3K/Akt/mTOR é uma via de sinalização intracelular importante na regulação do ciclo celular que responde a múltiplas questões nutricionais e ambientais. A desregulação dessa via está envolvida em múltiplas patologias humanas. A mTOR (*mechanistic target of rapamycin*) constitui a principal enzima que exerce o controle intermediário da via de sinalização e a sua ativação depende principalmente do acoplamento da subunidade mLst8 (*mammalian lethal with Sec13 protein 8*). Dada a importância da ligação mTOR-mLst8 no mecanismo de ativação da mTOR, à escassez de estudos direcionados a compreender o comportamento da quinase frente a esse acoplamento, a exploração das características da interação proteína-proteína na interface mTOR-mLst8 e o intuito de fornecer conhecimento para o desenvolvimento de novad estratégias de controle da via metabólica, neste trabalho empregamos dinâmica molecular com modelos *coarse-grained* para obter trajetórias do sistema mTOR-mLst8 a fim de avaliar as características da ligação mTOR-mLst8 e o perfil de ligação através de cálculos de energia livre, decomposição energética por resíduo e identificação de ligações de hidrogênio na interface mTOR-mLst8.

Palavras-chave

mTOR. mLst8. Modelos *coarse-grained*. Dinâmica molecular. Interação proteína-proteína. Perfil de ligação da interface mTOR-mLst8.

ABSTRACT

The PI3K/Akt/mTOR pathway is an important intracellular signaling pathway in cell cycle regulation that responds to multiple nutritional and environmental issues. Deregulation of this pathway is involved in multiple human pathologies. mTOR (*mechanistic target of rapamycin*) is the main enzyme that performs the intermediate control of the signaling pathway and its activation depends mainly on the binding of the mLst8 subunit (mammalian lethal with Sec13 protein 8). Due to the importance of the mTOR-mLst8 binding in the mTOR activation mechanism, the scarcity of studies aimed at understanding the kinase behavior regarding the binding, the exploration of the characteristics of the protein-protein interaction at the mTOR-mLst8 interface and the aim of providing knowledge for the development of new strategies to control the metabolic pathway, in this work we used molecular dynamics with coarse-grained models to obtain trajectories of the mTOR-mLst8 system in order to evaluate the characteristics of the mTOR-mLst8 binding and the binding profile through free energy calculations, energy decomposition per residue and identification of hydrogen bonds at the mTOR-mLst8 interface.

Keywords

mTOR. mLst8. Coarse-grained models. Molecular dynamics. Protein-protein interaction. mTOR-mLst8 interface binding profile.

LISTA DE ILUSTRAÇÕES

Figura 1. A via de sinalização PI3K/AKT/MTOR. 12
Figura 2. Diagrama estrutural da mTOR. 15
Figura 3. Esquema de mecanismo de fosfotransferência. 15
Figura 4. Mecanismo de ataque nucleofílico. 16
Figura 5. Processo de ativação da mTOR e fosforilação. 17
Figura 6. Estrutura molecular planar dos inibidores de primeira geração da mTOR. 19
Figura 7. Representação do mecanismo de inibição da mtor...................................20
Figura 8. Representação dos contatos FRB-FKBP12 com a rapamicina. 22
Figura 9. Mecanismo de ação da PROTAC. 25

SUMÁRIO

1 REVISÃO BIBLIOGRÁFICA 11
1.1 A via de sinalização PI3K/Akt/mTOR 11
1.2 Estrutura da quinase mTOR 13
1.3 Papel da subunidade mLst8 na ativação da mTOR 16
1.4 Processo de ativação secundário da mTOR 18
1.5 Mecanismo de inibição da via mTOR 19
1.6 Desafios dos inibidores de primeira geração e as inovações farmacológicas 22
1.7 Novas estratégias para controle de vias metabólicas 23
1.8 Compreendendo o comportamento do alvo 26
1.9 Desafios das metodologias de investigação do alvo 27
1.10 Aplicabilidade de métodos in silico no caso da mTOR 28
REFERÊNCIAS BIBLIOGRÁFICAS 29
2 OBJETIVOS 35
2.1 Objetivo Principal 35
2.2 Objetivos Específicos 35
3 RESULTADOS 36
3.1 Artigo I 36
3.2 Artigo II 56
4 CONCLUSÃO 77
5 PERSPECTIVAS 77
6 ANEXOS 79
6.1 Carta de aceite do Artigo I (DOI 10.1080/08927022.2021.1962525) 79
6.2 Carta de submissão do Artigo II 80

1 REVISÃO BIBLIOGRÁFICA

1.1 A via de sinalização PI3K/Akt/mTOR

A via PI3K/Akt/mTOR (Figura 1) é uma via de sinalização intracelular importante na regulação do ciclo celular que responde a múltiplas questões nutricionais e ambientais, incluindo fatores de crescimento, níveis de energia, estresse celular e aminoácidos. A tradução destes sinais leva à promoção do crescimento celular por fosforilação de substratos que desencadeiam processos anabólicos como a tradução de ácido ribonucleico mensageiro (ARNm) e a síntese lipídica, ou limitam processos catabólicos como a autofagia. Resumidamente, a dinâmica da via reside na ativação por meio de substratos extra/intracelulares da fosfatidilinositol-3 quinase (PI3K) que fosforila e ativa a proteína quinase B (AKT) localizada na membrana plasmática. A AKT, além de ser capaz de desencadear outros processos fosforilativos celulares, ativa a mTOR (*mechanistic target of rapamycin*) (PORTA; PAGLINO; MOSCA, 2014; SOLIMAN, 2013; ZAROGOULIDIS et al., 2014).

Devido a sua importância na integração de bioprocessos, a desregulação da via de sinalização, especialmente sua superexpressão, está implicada em um número crescente de condições patológicas, incluindo câncer, obesidade, diabetes tipo 2, neurodegeneração e envelhecimento precoce (LAPLANTE; SABATINI, 2012; SAXTON; SABATINI, 2017). Em todo o mundo, cerca de 19,3 milhões de novos casos e quase 10,0 milhões de mortes por câncer ocorreram em 2020 (SUNG et al., 2021). Em relação à obesidade, segundo a Organização Mundial da Saúde (OMS), em 2016, a prevalência foi de 13% da população adulta global (WORLD HEALTH ORGANIZATION, 2021). Em 2017, aproximadamente 462 milhões de indivíduos foram afetados pelo diabetes tipo 2, correspondendo a 6,28% da população mundial (4,4% dos 15-49 anos, 15% dos 50-69 anos e 22% dos 70+), ou uma taxa de prevalência de 6.059 casos por 100.000 (KHAN et al., 2020).

Figura 1. A via de sinalização PI3K/Akt/mTOR.

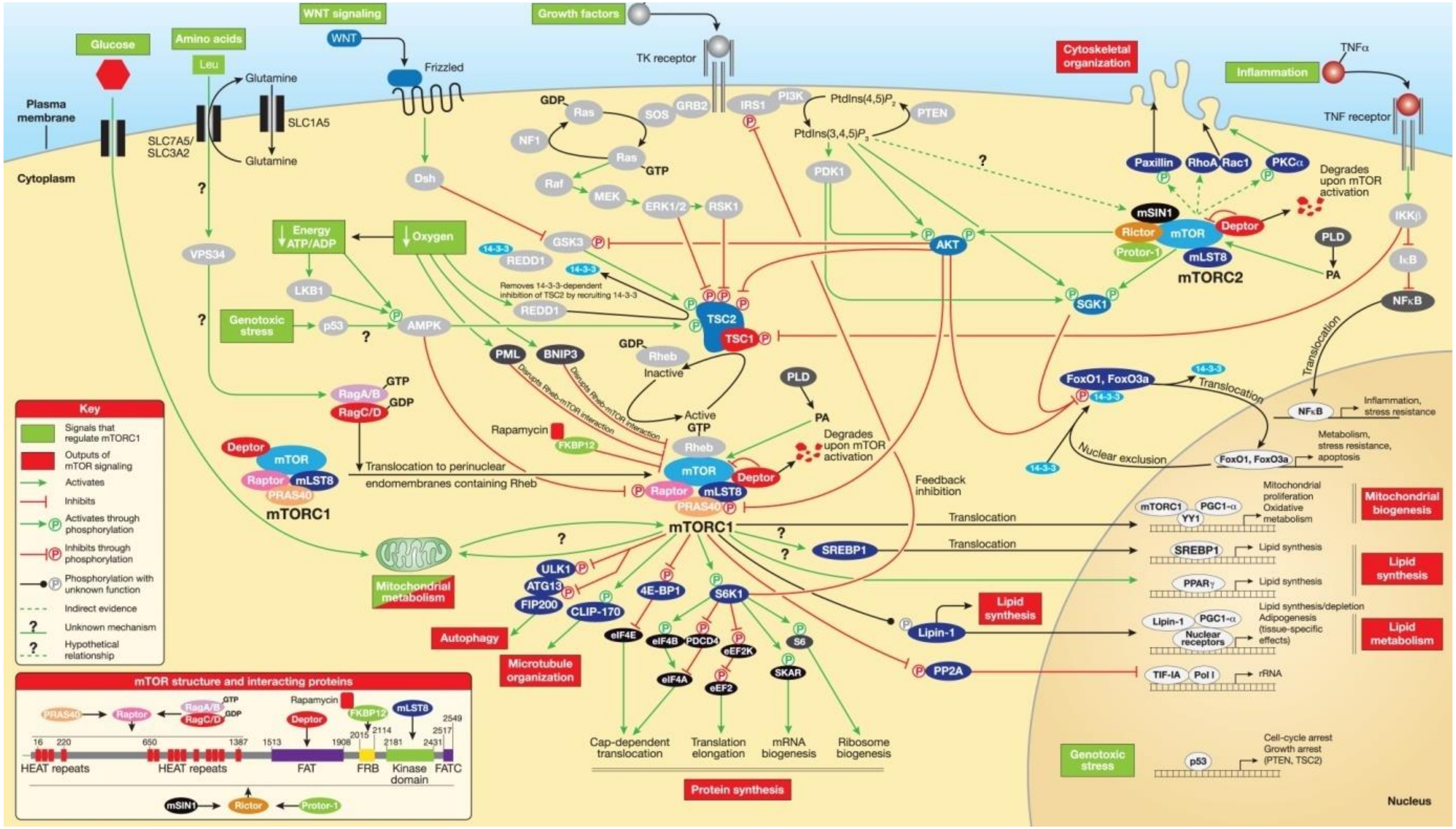

Adaptada de Laplante & Sabatini (2009).

1.2 Estrutura da quinase mTOR

A mTOR, formalmente denominada anteriormente de ser reconhecida como altamente conservada entre eucariotos como *mammalian Target Of Rapamycin* ou *FK506-binding protein 12-rapamycin-associated protein 1* (FRAP1), é uma quinase serina/treonina (EC 2.7.11.1) de 289 kDa pertencente à família das fosfatidilinositol-3 quinases (PI3K) e constitui a principal enzima que exerce o controle intermediário da via de sinalização também por meio do processo de fosfotransferência, possuindo a molécula de adenosina trifosfato (ATP) como doador de grupamentos fosfato (GUERTIN; SABATINI, 2007; LAPLANTE; SABATINI, 2009; SOLIMAN, 2013; YANG et al., 2013).

Estruturalmente, conforme a Figura 2, a quinase é composta de 2549 resíduos de aminoácidos que conta com um número distinto de domínios funcionais, incluindo (i) 32 repetições denominados *"Huntington, elongation factor 3, PR65/A, TOR"* (HEAT; do resíduo de aminoácido 17 ao 1260), (ii) um domínio *"FRAP, ATM, TRRAP"* (FAT; do resíduo de aminoácido 1261 ao 2001); (iii) um domínio catalítico e regulador *"kinase domain and regulatory domain"* (KD; do resíduo de aminoácido 2002 ao 2549) na porção C-terminal, o qual é formado por uma região N-terminal (do resíduo de aminoácido 2002 ao 2240) e uma região C-terminal (do resíduo de aminoácido 2241 ao 2549) assim como outras quinases canônicas eucarióticas. Na porção N-terminal do domínio KD, é encontrado o subdomínio (iv) *"FKBP12 rapamycin-binding"* (FRB; do resíduo de aminoácido 2021 ao 2118). Já o (v) elemento de ligação à subunidade mLst8 - *"mLst8 binding element"* (LBE; do resíduo de aminoácido 2258 ao 2296) está localizado na porção C-terminal, servindo como plataforma de ligação à mLst8. Além disso, na porção C-terminal da mTOR está situado o domínio (vi) *"FRAP ATM TRRAP carboxy terminus"* (FATC; do resíduo de aminoácido 2519 ao 2549). Conforme Figura 3, ainda no domínio KD da quinase, são encontrados os resíduos responsáveis pelo mecanismo de fosfotransferência: os resíduos Asn2343 e Asp2357, que servem de ligantes metálicos do cofator magnésio (Mg^{+2}) e o resíduo Asp2338, que desempenha um papel catalítico chave na orientação e ativação do grupo hidroxila do substrato para o ataque nucleofílico (Figura 4) (LAPLANTE; SABATINI, 2009, 2012; WATANABE; WEI; HUANG, 2011; YANG et al., 2013).

Esta quinase atípica está presente em dois complexos funcional e estruturalmente distintos, mTORC1 e mTORC2, localizados em diferentes compartimentos celulares, cada um contendo subunidades distintas e comuns necessárias à atividade e regulação catalíticas da enzima principal. O complexo mTORC1 – sensível à rapamicina – transmite sinais de disponibilidade de nutrientes para controlar crescimento celular e tradução proteica em parte por fosforilação da quinase S6 (S6K) e da eIF-4E binding protein 1 (SHOWKAT; BEIGH; ANDRABI, 2014; TEE; BLENIS, 2005), enquanto que o complexo mTORC2 – insensível à rapamicina – regula principalmente a montagem do citoesqueleto por actina por meio da fosforilação da proteína quinase C alfa (PKCα) e também pela fosforilação da Akt no motivo hidrofóbico (HM) (BETZ; HALL, 2013; LAPLANTE; SABATINI, 2012; SARBASSOV et al., 2004, 2005).

O complexo mTORC1 possui cinco componentes: mTOR, que é a subunidade catalítica do complexo; "*regulatory-associated protein of* mTOR" (Raptor) e "*mammalian lethal with Sec13 protein 8"* (mLst8 ou GβL) que são as subunidades regulatórias positivas; "*prolinerich AKT substrate 40 kDa"* (PRAS40) e "*DEP-domain-containing mTOR-interacting protein"* (Deptor), que são as subunidades regulatórias negativas (HARA et al., 2002; KIM et al., 2003; LAPLANTE; SABATINI, 2009; VANDER HAAR et al., 2007; YANG et al., 2013; ZHAO; XIONG; SUN, 2011). Já o mTORC2 é composto por seis subunidades proteicas: algumas comuns à mTORC1 e mTORC2: mTOR; "*rapamycin-insensitive companion of* mTOR" (Rictor); "*mammalian stress-activated protein kinase interacting protein"* (mSIN1) e "*protein observed with* Rictor-1" (Protor-1) que desempenham o papel de estabilizar o complexo formado; mLst8; e Deptor (FRIAS et al., 2006; KIM et al., 2003; LAPLANTE; SABATINI, 2009; PEARCE et al., 2007; SARBASSOV et al., 2004; YANG et al., 2013; ZHAO; XIONG; SUN, 2011) .

Figura 2. Diagrama estrutural da mTOR.

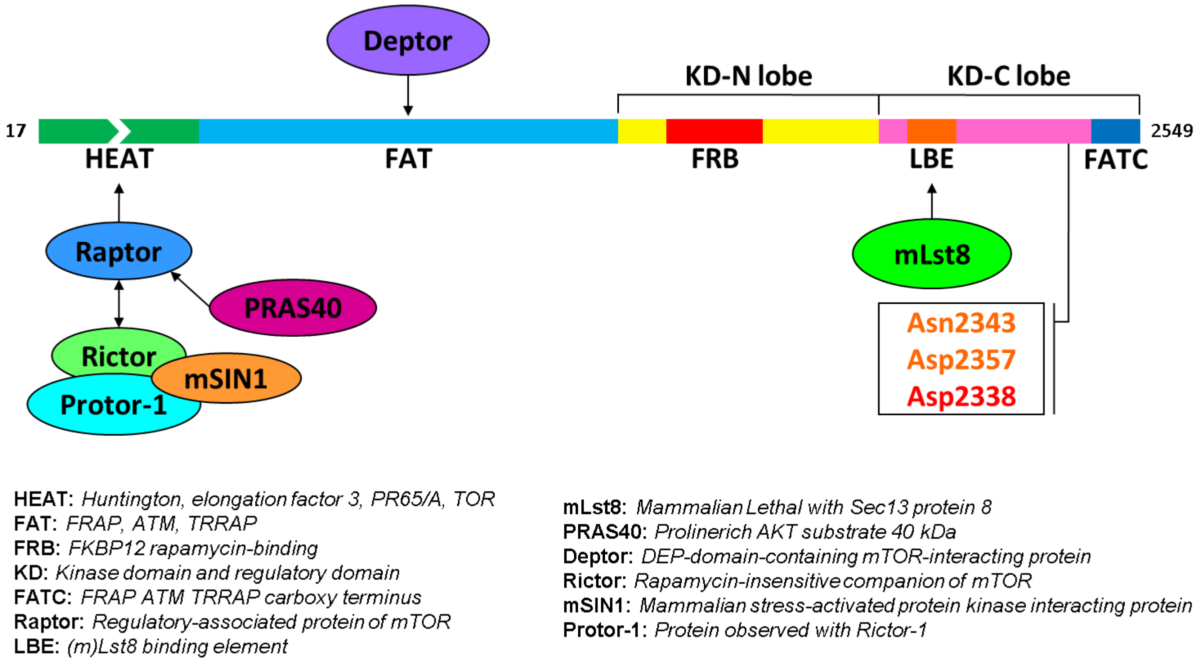

Fonte: Elaborada pelo autor.

Figura 3. Esquema de resíduos e cofator envolvidos no mecanismo de fosfotransferência.

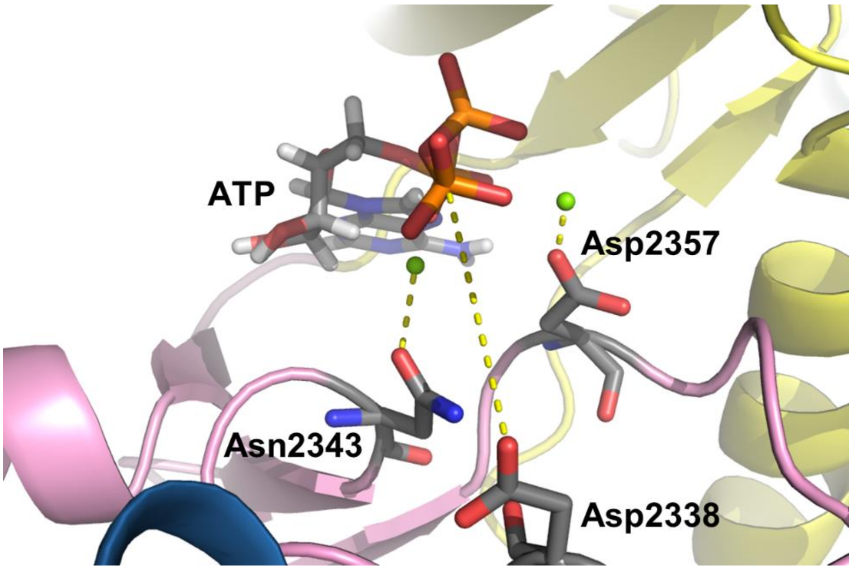

Átomos de Mg^{+2}, em esferas verdes, resíduos e ATP representados na forma de palitos e restante das frações proteicas em representação de *cartoon*.

Fonte: Elaborada pelo autor.

Figura 4. Mecanismo de ataque nucleofílico.

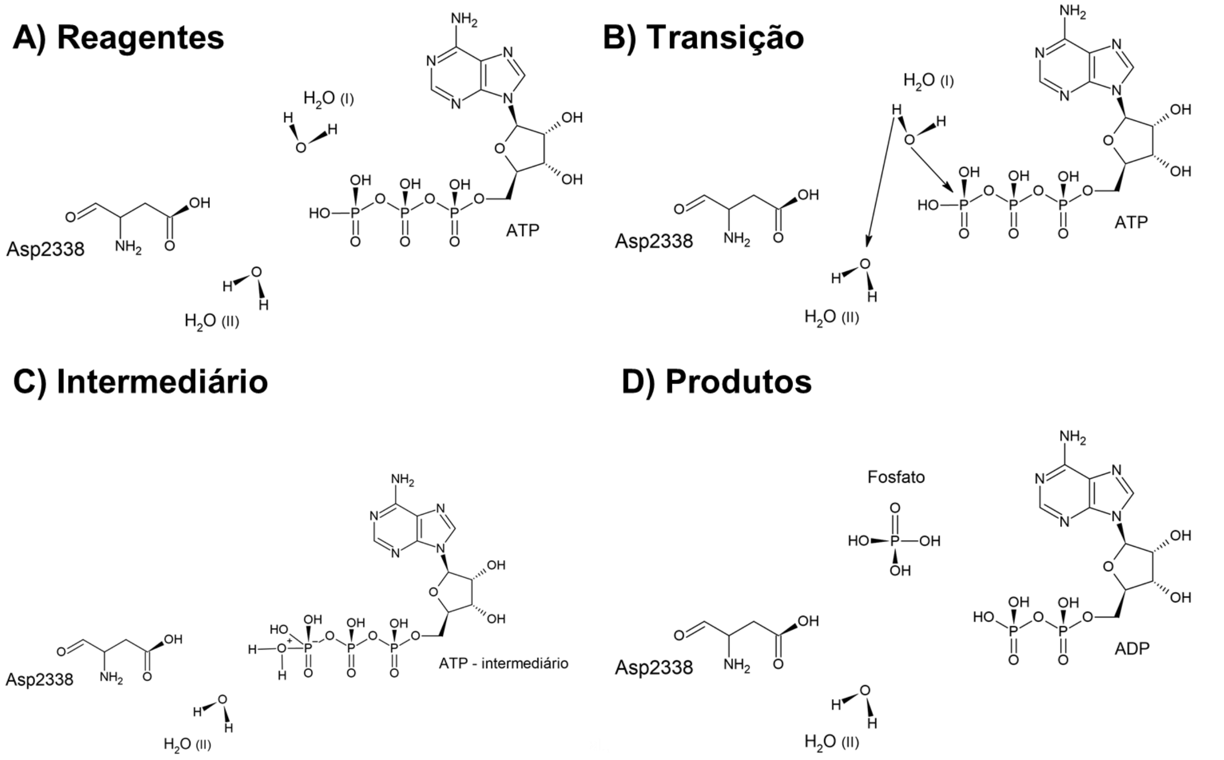

Fonte: Elaborada pelo autor.

1.3 Papel da subunidade mLst8 na ativação da mTOR

Os mecanismos moleculares subjacentes à regulação da atividade do mTOR foram elucidados por uma estrutura do complexo de mTOR e a subunidade mLst8 (YANG et al., 2013). A mLst8 é uma subunidade comum de ambos os complexos, mTORC1 e mTORC2, e a acoplagem desta subunidade é necessária para a ativação da mTOR. Para tal processo, conforme a Figura 5, a quinase mTOR (5A) é acoplada pela porção mLst8 (5B) fazendo com que haja uma mudança conformacional com posterior exposição do sítio fosforilativo (5C). Neste momento, dois átomos de magnésio (5D) orientam a entrada de ATP para subsequente hidrólise (5E) (LAPLANTE; SABATINI, 2009; WATANABE; WEI; HUANG, 2011; YANG et al., 2013)

A estrutura do complexo mTOR-mLst8 revelou que a mLst8 estabiliza diretamente o sítio ativo da mTOR, apoiando a ideia de que a fração mLst8 desempenha um papel crítico na atividade dessa quinase cujas análises de embriões e fibroblastos de camundongos mLst8-knockout mostraram que mLst8 é necessária para a formação do complexo mTOR e sua ativação (GUERTIN et al., 2006). Dessa forma, a fração mLst8 é crítica para a regulação adequada de ambos os complexos da mTOR, mas sua função ainda precisa ser definida. Além disso, a contribuição de mLst8 para o desenvolvimento de patologias, particularmente aquelas em que as vias mTOR são desreguladas, permanece descaracterizada.

Figura 5. Processo de ativação da mTOR e fosforilação.

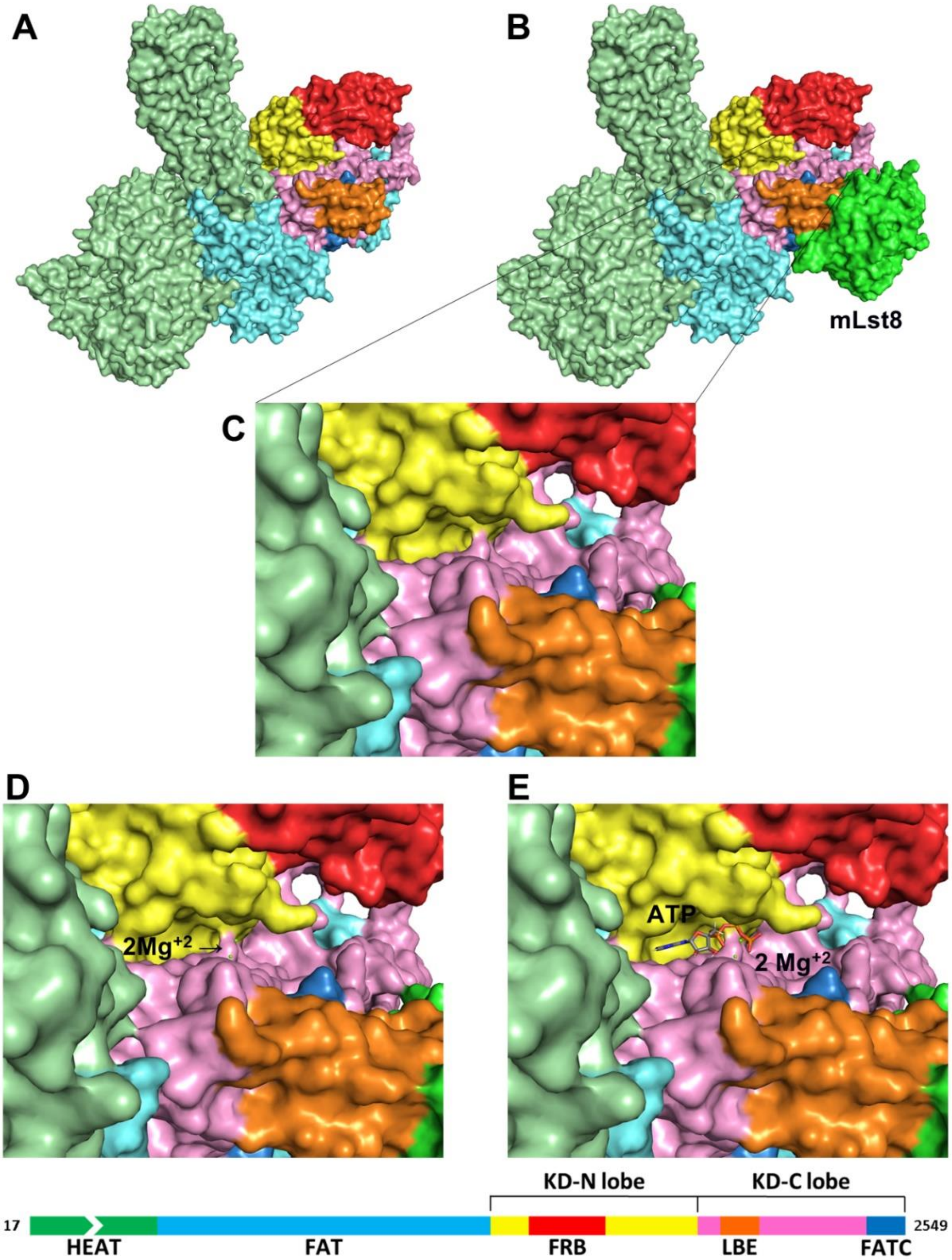

Fonte: Elaborada pelo autor utilizando PDBID 6BCU.

1.4 Processo de ativação secundário da mTOR

Aparentemente, após a ligação mTOR-mLst8, há o desencadeamento de diversos processos de fosforilação a fim de tornar a quinase ativa, tornando o mecanismo complexo. Sabe-se que existem 4 sítios de fosforilação caracterizados na mTOR, incluindo a Ser1261, a Thr2446, a Ser2448 e a Ser2481 (WATANABE; WEI; HUANG, 2011).

A Ser1261, do domínio HEAT, é fosforilada pela insulina/fosfatidilinositol 3-quinase (PI3K) de maneira dependente de aminoácidos, insensível à rapamicina e independente de autofosforilação. A fosforilação de Ser1261 promove a fosforilação de S6K e 4E-BP1 e a mutação em Ser1261 atenua a fosforilação em Ser2481. O resíduo Thr2446 é fosforilado em resposta à disponibilidade de nutrientes e provavelmente é fosforilado pela adenosina monofosfato quinase (AMPK) (CHENG et al., 2004). Inicialmente, relatou-se que o resíduo Ser2448 é um sítio de fosforilação da Akt porque sua fosforilação é sensível à inibição da quinase PI-3 (PI-3K) que reduz a atividade da Akt. No entanto, relatos mais recentes mostraram que a S6K é a própria quinase Ser2448 (CHIANG; ABRAHAM, 2005; HOLZ; BLENIS, 2005). O resíduo Ser2481 é um sítio de autofosforilação insensível à rapamicina (PETERSON et al., 2000). Relata-se que as mutações de Thr2446 e Ser2448 para alanina não tem efeito perceptível na capacidade da mTOR de ativar seus efetores a jusante. No entanto, o fato de que a deleção interna dos resíduos 2430-2450 aumenta a atividade da quinase da mTOR e isso sugere que essa região é reguladora (SEKULIĆ et al., 2000). Atualmente, o significado funcional da fosforilação da mTOR nesses locais ainda não foi totalmente explorado e permanece pouco compreendido.

Embora experimentos de Copp e colaboradores (2009), Acosta-Jaquez e colaboradores (2009) e Tao e colaboradores (2010) demonstraram que a mTOR, tanto no complexo mTORC1 quanto no complexo mTORC2, é fosforilada em diferentes locais e que a fosforilação de mTOR é mais complexa do que se pensava anteriormente (ACOSTA-JAQUEZ et al., 2009; COPP; MANNING; HUNTER, 2009; TAO et al., 2010) ainda são necessárias abordagens para comprender o processo de fosfotransferência da quinase mTOR explorando o sítio de ligação do ATP e quantificando as barreiras energéticas da reação enzimática.

1.5 Mecanismo de inibição da via mTOR

A inibição clássica da via da mTOR é efetuada pela rapamicina e seus derivados análogos, denominados *rapalogs*, que são considerados os inibidores de primeira geração (Figura 6) (ABRAHAM T.; GIBBONS; GRAZIANI I., 2010; SANTULLI; TOTARY-JAIN, 2013; SEHGAL, 2003; ZHENG; JIANG, 2015).

Figura 6. Estrutura molecular planar dos inibidores de primeira geração da mTOR.

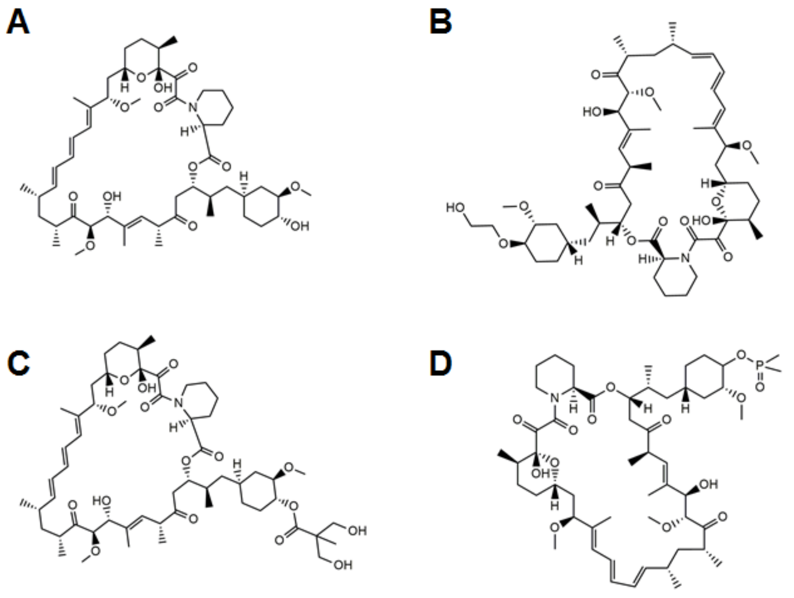

(A) rapamicina/sirolimo, (B) everolimo, (C) temsirolimo e (D) deforolimo.
Fonte: Elaborada pelo autor.

A rapamicina ou sirolimo (Rapamune, Wyeth Pharmaceuticals), CAS 53123-88-9, fórmula molecular $C_{51}H_{79}NO_{13}$ e massa molecular de 914,17 g/mol, foi descoberta na Ilha da Páscoa, Chile, em 1972. Trata-se de um potente antibiótico macrolídeo produzido pelo micro-organismo *Streptomyces higroscopicus* e que, por possuir propriedades antifúngica, imunossupressora e antitumoral, é utilizado amplamente na terapêutica. Todavia, devido a suas propriedades desfavoráveis, como a sua baixa solubilidade em água e estabilidade em solução, foram desenvolvidos análogos moleculares, os *rapalogs*, como o everolimo (RAD001, Afinitor, Novartis Pharmaceuticals), temsirolimo (CCI-779, Torisel, Wyeth Pharmaceuticals) e ridaforolimo (AP23573; formalmente deforolimo, ARIAD Pharmaceuticals), os quais melhoraram as propriedades farmacocinéticas sem alterar o mecanismo de ação (SANTULLI; TOTARY-JAIN, 2013).

O mecanismo de inibição da mTOR pela rapamicina e seus análogos reside na ligação ao receptor intracelular da *FK506-binding protein 12 kDa* (FKBP12), formando o complexo rapamicina-FKBP12 que se liga direta e predominantemente ao domínio *FKBP12-rapamycin binding* (FRB), bloqueando de forma alostérica o sítio catalítico de fosforilação conforme demonstrado na Figura 7 (LAPLANTE; SABATINI, 2009; SHIMOBAYASHI; HALL, 2014; YANG et al., 2013).

Figura 7. Representação do mecanismo de inibição da mTOR.

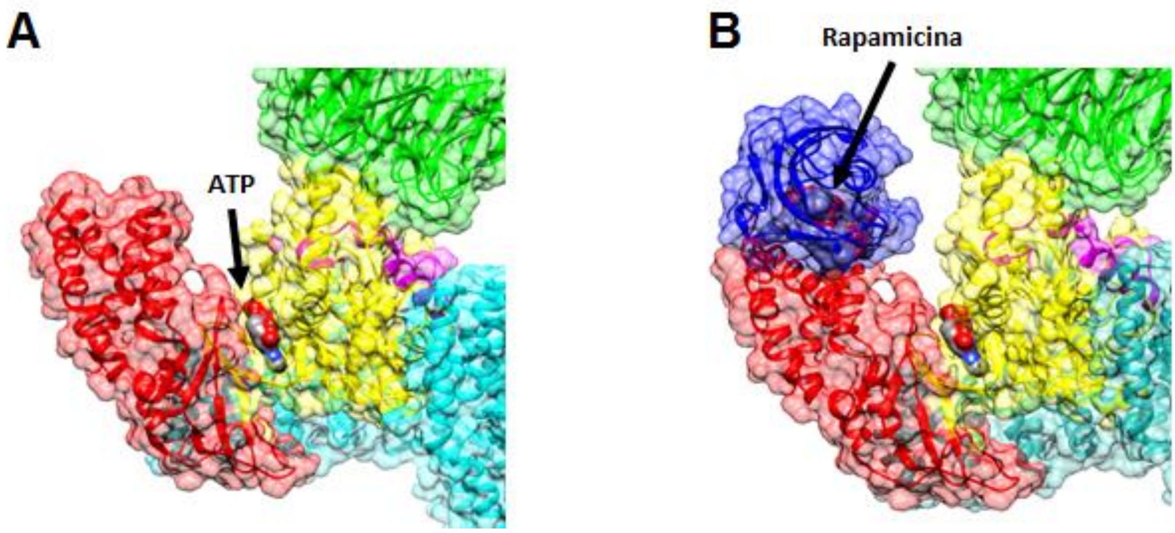

A) Representação da superfície da estrutura do complexo mTOR-mLst8-ATP; B) Representação da superfície da estrutura do modelo mTOR-mLst8-ATP-rapamicina-FKBP12. Em ciano, domínio FAT; em vermelho, domínio FRB; em amarelo, domínio quinase; em magenta, domínio FATC; em verde, subunidade proteica mLst8; em azul, a subunidade proteica FKBP12.

Fonte: Elaborada pelo autor utilizando o programa Chimera v.1.9 (PETTERSEN et al., 2004), baseando-se em Yang e colaboradores (2013) (YANG et al., 2013) nos modelos PDBID 1FAP e 4JSP.

Na prática, a partir de experimentos de Banaszynski e colaboradores (2005) revelou-se a constante de dissociação (K_d) moderadamente favorável entre a rapamicina e FRB (K_d = 26 ± 0,8 μM). No entanto, o complexo rapamicina-FKBP12 associa-se à FRB com uma afinidade 2000 vezes maior (K_d = 12 ± 0,8 nM) do que a rapamicina por si só. Além disso, nenhuma interação entre FKBP12 e FRB foi detectada na ausência de rapamicina. Assim, sugere-se que a capacidade da rapamicina em se ligar à fração FRB e, por extensão, à mTOR na ausência de FKBP12, é de pouca importância sob condições fisiológicas. Além do mais, as interações proteína-proteína na interface FRB-FKBP12 desempenham um papel fundamental na estabilidade do complexo ternário (BANASZYNSKI; LIU; WANDLESS, 2005).

A Figura 8 ilustra as interações entre os resíduos proteicos da porção FRB (do resíduo 108 a 201) e da porção FKBP12 (do resíduo 1 a 107) com a molécula de rapamicina. Adotou-se como parâmetros para ligação de hidrogênio, em angstroms (Å): distância máxima hidrogênio-aceptor de 3,2 Å e doador-aceptor de 4,0 Å; distância de contato mínima e máxima de 3,6 Å somente para contatos hidrofóbicos. Identifica-se interações hidrofóbicas com a porção FRB (cadeia B) nos resíduos Ser124, Phe128, Gly129, Thr187, Trp190 e Tyr194; interações hidrofóbicas com a porção FKBP12 (cadeia A) nos resíduos Phe36, Phe46, Val55, Trp59, Ile90; interações do tipo ligações de hidrogênio apenas com a porção FKBP12 (cadeia A) em Asp37 (2,76 Å); Gln53 (2,62 Å); Glu54 (2,88 Å); Ile56 (2,78 Å) e Tyr82 (2,71 Å).

Figura 8. Representação dos contatos FRB-FKBP12 com a rapamicina.

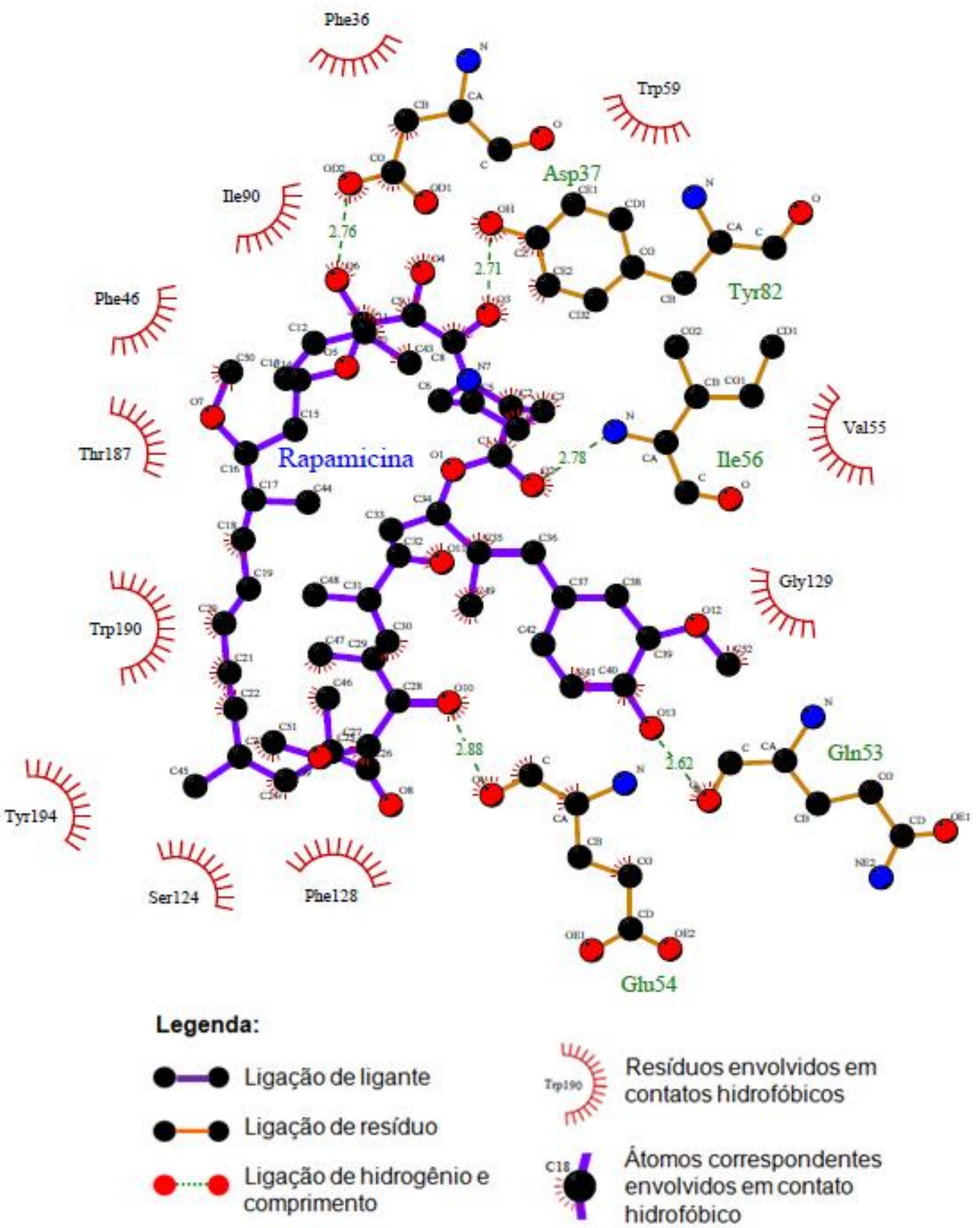

Resíduos proteicos de FKBP12 (do resíduo 1 ao 107) e FRB (do resíduo 108 ao 202) que realizam interações com uma molécula de rapamicina.

Fonte: Elaborada pelo autor utilizando o programa LigPlot^{+} v.1.4 (LASKOWSKI; SWINDELLS, 2011).

1.6 Desafios dos inibidores de primeira geração e as inovações farmacológicas

Os *rapalogs* revelaram eficácia, segurança e tolerabilidade de eventos adversos na inibição da via da mTOR em uma série de estudos. Contudo, o sucesso desses inibidores de primeira geração tem demonstrado falhas especialmente devido ao mecanismo de *feedback*, já que a inibição do complexo resulta na hiperativação da sinalização PI3K/Akt e incrementa a sobrevivência celular; além disso, determinada insensibilidade do mTORC1 aos *rapalogs* foi recentemente revelada, desafiando o dogma de que a rapamicina inibe completamente a atividade do mTORC1; vias alternativas e cruzamento de vias entre as quinases também poderiam limitar a eficácia dos *rapalogs* e mutações na via PI3K/Akt/mTOR (CARRACEDO; PANDOLFI, 2008; CHOO et al., 2008; CHOO; BLENIS, 2009; DI NICOLANTONIO et al., 2010; GUERTIN; SABATINI, 2009; SANTULLI; TOTARY-JAIN, 2013; THOREEN et al., 2009; WACHECK, 2010).

Dessa forma, o esforço recente tem se baseado na busca por inibidores diretos do sítio catalítico de quinases, ou seja, ATP-competitivos. Nesse caso, pode-se citar fármacos com testes clínicos já iniciados como os inibidores duplos de segunda geração – mTOR/PI3K *dual inhibitors* (TPdIs) como, por exemplo, PF-0469150212, BEZ23513 e GSK212645814 e seletivos mTORC1/mTORC2 *dual inhibitors* (TORCdIs) como, por exemplo, OSI-0279, INK-12810 e CC-22311 (BHAGWAT et al., 2011; GUO; KWIATKOWSKI, 2013; KNIGHT et al., 2010; MUKHERJEE et al., 2012; SANTULLI; TOTARY-JAIN, 2013; YUAN et al., 2011; ZASK; VERHEIJEN; RICHARD, 2011; ZHENG; JIANG, 2015).

Apesar de demonstrar certa seletividade e grande promessa na terapêutica, a maioria dos inibidores de quinases não são seletivos a um único alvo molecular. Tal fato aumenta potencialmente o risco de efeitos indesejáveis e toxicidade devido à interação com outras enzimas e à inibição de outras quinases essenciais ao metabolismo. Dessa forma, é importante a busca por inibidores cada vez mais seletivos a determinados alvos (LUO, 2005; SMITH; SIMONS, 2004; THAIMATTAM et al., 2007; WANG et al., 2016).

1.7 Novas estratégias para controle de vias metabólicas

O desenvolvimento de novos fármacos visa à identificação de compostos de interesse farmacológico e de estratégias terapêuticas que atendam tanto o tratamento de doenças quanto a melhoria da qualidade de vida do paciente. Até há pouco tempo, candidatos a fármacos eram descritos como moléculas orgânicas que geralmente compartilham características físico-químicas semelhantes. Atualmente, sabe-se que as interações proteína-proteína (PPIs) em vias metabólicas são essenciais para ativação ou inibição de processos fisiopatológicos. Dessa forma, o grande desafio é compreender como as proteínas podem interagir entre si nas vias metabólicas e quais são as características dessas ligações para descobrir novos potenciais moduladores das PPIs na intervenção terapêutica (CICALONI et al., 2019; PENG et al., 2016).

No que diz respeito à redução de custos e tempo, as técnicas computacionais são muito úteis para auxiliar o conhecimento sobre PPIs, pois podem empregar uma estrutura proteica resolvida de um banco de dados, auxiliar na modelagem de estruturas faltantes, realizar simulações de dinâmica molecular para elucidar o comportamento das PPIs e avaliar os resultados com análise estatística a fim de verificar a eficácia e precisão do método (CICALONI et al., 2019; PENG et al., 2016). Tanto que nos últimos anos, foram encontradas algumas soluções terapêuticas baseadas em PPIs como, por exemplo, a tecnologia denominada *"proteolysis targeting chimeric"* (PROTAC) – um mecanismo eficaz de degradação de proteínas endógenas de interesse farmacológico (POI) através do sistema ubiquitina-proteassoma (UPS) que visa impedir a ativação ou inibição de determinada cascata metabólica (GAO; SUN; RAO, 2020; GU et al., 2018; HE et al., 2020; PEI et al., 2019; PETTERSSON; CREWS, 2019; QI et al., 2021; SUN et al., 2019).

Conforme a Figura 9, o mecanismo de ação da tecnologia PROTAC envolve (i) o desenvolvimento da PROTAC em si através da união de um ligante da POI com um ligante de ubiquitina E3 ligase por meio de um *linker* (uma pequena molécula), (ii) a formação de um complexo ternário entre a POI, PROTAC e a ubiquitina E3 ligase, (iii) a poliubiquitinação da POI com a reciclagem da PROTAC e (iv) a degradação da POI via sistema proteassoma com a formação de resíduos de aminoácidos (GU et al., 2018).

Figura 9. Mecanismo de ação da PROTAC.

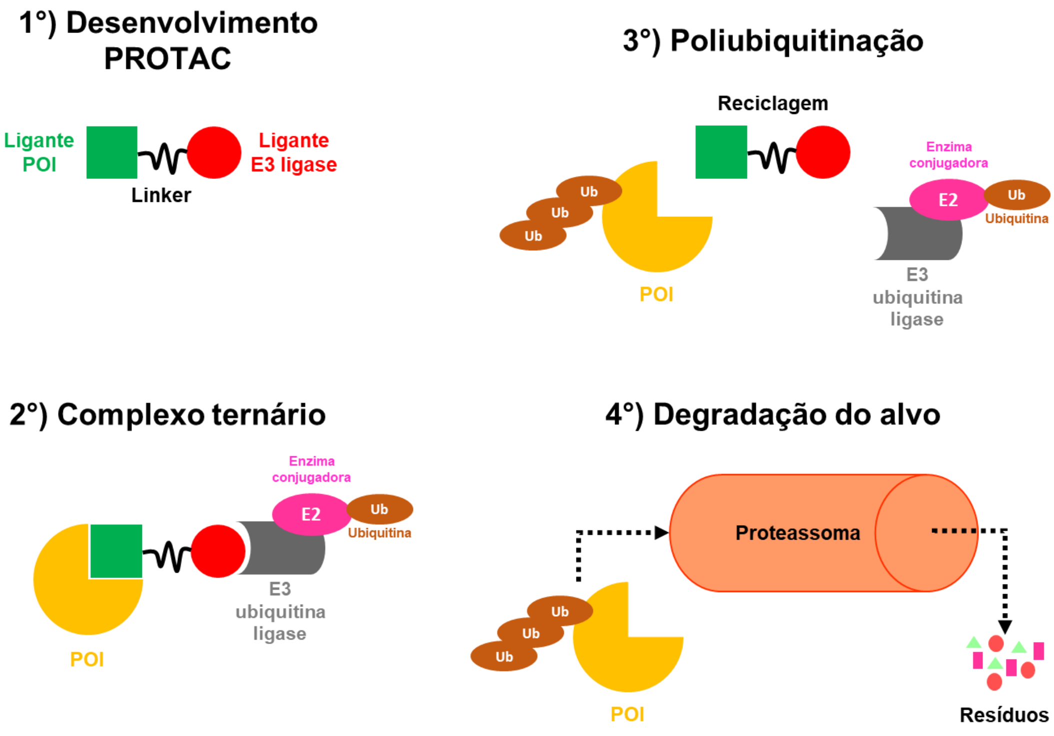

Fonte: Elaborada pelo autor.

As principais vantagens desta tecnologia são reduzir os efeitos adversos indesejáveis devido a especificidade ao alvo, reduzir a toxicidade e a dose-resposta em relação aos tratamentos convencionais uma vez que há a reciclagem da PROTAC no sistema, reduzir a resistência ao alvo e ser uma solução para alvos que não respondem a fármacos convencionais (GAO; SUN; RAO, 2020; GU et al., 2018; HE et al., 2020; PEI et al., 2019; PETTERSSON; CREWS, 2019; QI et al., 2021; SUN et al., 2019). Atualmente, há pelo menos 15 PROTACs nos primeiros estágios de pesquisa clínica e alguns deles já chegam à clínica com perfis satisfatórios de segurança e eficácia (AMBROSINI et al., 2022; FLANAGAN et al., 2019; MULLARD, 2019, 2020, 2021; PETRYLAK et al., 2020).

1.8 Compreendendo o comportamento do alvo

Visto que proteínas são biomoléculas complexas que, em geral, demonstram uma ampla dinâmica envolvida na atividade e controle de vias metabólicas e que há necessidade de entender tais processos dinâmicos, no desenvolvimento de fármacos por computação assistida emprega-se uma ferramenta importante denominada simulação computacional por dinâmica molecular (DM). Tal técnica permite determinar os movimentos das partículas de qualquer sistema do qual se conheçam o potencial de interação entre essas partículas e as equações que regem seu movimento. Dessa forma, possibilita a evolução temporal das configurações dos constituintes do sistema e, por intermédio das sequências de posições geradas, determinam-se as propriedades macroscópicas do sistema de acordo com os princípios de Mecânica Estatística (MARTÍNEZ; BORIN; SKAT, 2007; NAMBA; DA SILVA; DA SILVA, 2008).

Nessa metodologia, partículas interagentes, inicialmente dispostas em uma configuração, movimentam-se sob a influência de potenciais intermoleculares. De posse dos dados relativos às posições e velocidades de todas as partículas envolvidas em um dado instante (t_0), pode-se computar as forças resultantes em cada partícula devido à interação com as demais e determinar posições e velocidades em um tempo posterior ($t_0 + \delta t$) por meio de equações de movimento Newtonianas. As novas posições são utilizadas para a computação de novas forças e posteriores posições e velocidades em ($t_0 + 2\delta t$). Tal procedimento é realizado recursivo e intermitentemente gerando trajetórias moleculares para todo o sistema (MARTÍNEZ; BORIN; SKAT, 2007; NAMBA; DA SILVA; DA SILVA, 2008).

Existem múltiplos fatores envolvidos na técnica de simulação por DM de macromoléculas, entre os quais a complexidade do sistema a ser compreendido torna-se o principal fator que influencia no tempo total da simulação. Esses fatores, como o cálculo das forças exercidas sobre cada partícula do sistema devido às interações intermoleculares; a movimentação das partículas; o estabelecimento dos protocolos e dos controles de simulação, a análise ou armazenamento das configurações devem ser cuidadosamente planejados e previamente avaliados para se obter resultados satisfatórios (MARTÍNEZ; BORIN; SKAT, 2007; NAMBA; DA SILVA; DA SILVA, 2008).

1.9 Desafios das metodologias de investigação do alvo

Destaca-se que a complexidade estrutural e dinâmica das vias metabólicas são fatores que influenciam diretamente na concepção de conhecimento aplicado sobre determinado alvo molecular. Por exemplo, no caso da mTOR, através de estudos prévios do processo inibitório, conseguimos propor novas estratégias de inibição da via de sinalização (KIST; CACERES, 2016; KIST; TIMMERS; CACERES, 2018). Contudo, o conhecimento sobre o mecanismo de ativação ainda é desconhecido e gera curiosidade sobre sua complexidade uma vez que a ativação da enzima principal depende de acoplamentos de subunidades proteicas e, inclusive, de processos fosforilativos secundários para tornar a quinase competente para que a hidrólise do ATP no sítio catalítico ocorra adequadamente. Aliado a essa problemática, devemos considerar o tamanho do sistema que, apenas para a mTOR, são mais de 2500 resíduos de aminoácidos que tornam a abordagem atomística do sistema praticamente inviável.

Por meio de estudos teóricos e experimentais, sabe-se que estruturas proteicas secundárias e outras características geométricas das cadeias de proteínas reduzem o número de conformações disponíveis e, portanto, facilitam o enovelamento das estruturas terciárias nativas. Dessa forma, é possível compreender o comportamento de biomoléculas complexas e de grandes dimensões por meio de modelos de *coarse-grained* (CG) que elevam o nível de resolução do sistema e reduzem o tempo de simulação (KMIECIK et al., 2016).

Dentre vários modelos disponíveis, o SIRAH (Southamerican Initiative for a Rapid and Accurate Hamiltonian) é uma ferramenta que proporciona um campo de força para simulações de proteínas em meio aquoso e que também possui a resolução de campo de força para o ATP, tornando factível o entendimento do comportamento de quinases complexas (DARRÉ et al., 2015).

1.10 Aplicabilidade de métodos *in silico* no caso da mTOR

O primeiro passo para desenvolver novas estratégias de controle de vias metabólicas, seja por inibição clássica por fármacos por meio de triagem virtual de pequenas moléculas ou por interações proteína-proteína, é entender o comportamento do alvo. Dessa forma, focamos em investigar o impacto da ligação mTOR-mLst8 no comportamento da quinase e as características da interface mTOR-mLst8, uma vez que a ativação da quinase depende da ligação da subunidade mLst8 (GUERTIN et al., 2006; YANG et al., 2013). Portanto, essa característica por si só já demonstra seletividade ao alvo, pois não há ativação da quinase e subsequente superexpressão da via sem ligação mTOR-mLst8 e, embora a complexa via mTOR seja crucial para muitos processos biológicos, não há muitos estudos explorando a interface e o acoplamento mTOR-mLst8 em nível molecular para ativação da via de sinalização.

Na literatura, a única caracterização da interação mTOR-mLst8 foi realizada por Santos de Oliveira e colaboradores (2020) que não descreve o comportamento da quinase e apenas sugere a relevância de determinados resíduos da interface mTOR-mLst8 na ligação proteína-proteína (SANTOS DE OLIVEIRA et al., 2020).

Assim, o comportamento da mTOR diante de seu mecanismo de ativação tendo o acoplamento mLst8-mTOR como primordial à atividade fosforilativa, se torna um campo fértil de conhecimento e descoberta de novas estratégias terapêuticas.

REFERÊNCIAS BIBLIOGRÁFICAS

ABRAHAM T., R.; GIBBONS, J. J.; GRAZIANI I., E. Chemistry and Pharmacology of Rapamycin and Its Derivatives. In: HALL, M. N.; TAMANOI, F. (Eds.). . **The Enzymes: Structure, Function and Regulation of TOR complexes from Yeasts to Mammals.** [s.l.] Academic Press, 2010. v. 27p. 329–356.

ACOSTA-JAQUEZ, H. A. et al. Site-Specific mTOR Phosphorylation Promotes mTORC1-Mediated Signaling and Cell Growth. **Molecular and Cellular Biology**, v. 29, n. 15, p. 4308–4324, 8 jan. 2009.

ADMIRAAL, S. J.; HERSCHLAG, D. Mapping the transition state for ATP hydrolysis: implications for enzymatic catalysis. **Chemistry & biology**, v. 2, n. 11, p. 729–739, 1995.

AMBROSINI, M. et al. Targeted protein degraders from an oncologist point of view: The Holy Grail of cancer therapy? **Critical Reviews in Oncology/Hematology**, v. 169, p. 103532, 1 jan. 2022.

BANASZYNSKI, L. A.; LIU, C. W.; WANDLESS, T. J. Characterization of the FKBP.rapamycin.FRB ternary complex. **J Am Chem Soc**, v. 127, n. 13, p. 4715–4721, 2005.

BETZ, C.; HALL, M. N. Where is mTOR and what is it doing there? **J Cell Biol**, v. 203, n. 4, p. 563–574, 2013.

BHAGWAT, S. V. et al. Preclinical characterization of OSI-027, a potent and selective inhibitor of mTORC1 and mTORC2: distinct from rapamycin. **Mol Cancer Ther**, v. 10, n. 8, p. 1394–1406, 2011.

CARRACEDO, A.; PANDOLFI, P. P. The PTEN-PI3K pathway: of feedbacks and cross-talks. **Oncogene**, v. 27, n. 41, p. 5527–5541, 2008.

CHENG, S. W. Y. et al. Thr2446 is a novel mammalian target of rapamycin (mTOR) phosphorylation site regulated by nutrient status. **The Journal of Biological Chemistry**, v. 279, n. 16, p. 15719–15722, 16 abr. 2004.

CHIANG, G. G.; ABRAHAM, R. T. Phosphorylation of mammalian target of rapamycin (mTOR) at Ser-2448 is mediated by p70S6 kinase. **The Journal of Biological Chemistry**, v. 280, n. 27, p. 25485–25490, 8 jul. 2005.

CHOO, A. Y. et al. Rapamycin differentially inhibits S6Ks and 4E-BP1 to mediate cell-type-specific repression of mRNA translation. **Proc Natl Acad Sci U S A**, v. 105, n. 45, p. 17414–17419, 2008.

CHOO, A. Y.; BLENIS, J. Not all substrates are treated equally: implications for mTOR, rapamycin-resistance and cancer therapy. **Cell Cycle**, v. 8, n. 4, p. 567–572, 2009.

CICALONI, V. et al. Applications of in Silico Methods for Design and Development of Drugs Targeting Protein-Protein Interactions. **Current Topics in Medicinal Chemistry**, v. 19, n. 7, p. 534–554, 2019.

COPP, J.; MANNING, G.; HUNTER, T. TORC-specific phosphorylation of mTOR: phospho-Ser2481 is a marker for intact mTORC2. **Cancer research**, v. 69, n. 5, p. 1821–1827, 1 mar. 2009.

DARRÉ, L. et al. SIRAH: A Structurally Unbiased Coarse-Grained Force Field for Proteins with Aqueous Solvation and Long-Range Electrostatics. **Journal of Chemical Theory and Computation**, v. 11, n. 2, p. 723–739, fev. 2015.

DI NICOLANTONIO, F. et al. Deregulation of the PI3K and KRAS signaling pathways in human cancer cells determines their response to everolimus. **J Clin Invest**, v. 120, n. 8, p. 2858–2866, 2010.

FLANAGAN, J. et al. Abstract P5-04-18: ARV-471, an oral estrogen receptor PROTAC degrader for breast cancer. 2019.

FRIAS, M. A. et al. mSin1 is necessary for Akt/PKB phosphorylation, and its isoforms define three distinct mTORC2s. **Current biology: CB**, v. 16, n. 18, p. 1865–1870, 19 set. 2006.

GAO, H.; SUN, X.; RAO, Y. PROTAC Technology: Opportunities and Challenges. **ACS Medicinal Chemistry Letters**, v. 11, n. 3, p. 237–240, 12 mar. 2020.

GU, S. et al. PROTACs: An Emerging Targeting Technique for Protein Degradation in Drug Discovery. **BioEssays**, v. 40, n. 4, p. 1700247, 2018.

GUERTIN, D. A. et al. Ablation in mice of the mTORC components raptor, rictor, or mLST8 reveals that mTORC2 is required for signaling to Akt-FOXO and PKC alpha but not S6K1. **Dev Cell**, v. 11, 2006.

GUERTIN, D. A.; SABATINI, D. M. Defining the role of mTOR in cancer. **Cancer Cell**, v. 12, n. 1, p. 9–22, 2007.

GUERTIN, D. A.; SABATINI, D. M. The pharmacology of mTOR inhibition. **Sci Signal**, v. 2, n. 67, p. pe24, 2009.

GUO, Y.; KWIATKOWSKI, D. J. Equivalent benefit of rapamycin and a potent mTOR ATP-competitive inhibitor, MLN0128 (INK128), in a mouse model of tuberous sclerosis. **Mol Cancer Res**, v. 11, n. 5, p. 467–473, 2013.

HARA, K. et al. Raptor, a binding partner of target of rapamycin (TOR), mediates TOR action. **Cell**, v. 110, n. 2, p. 177–189, 2002.

HE, Y. et al. Proteolysis targeting chimeras (PROTACs) are emerging therapeutics for hematologic malignancies. **Journal of Hematology & Oncology**, v. 13, n. 1, p. 103, 27 jul. 2020.

HERSCHLAG, D.; JENCKS, W. P. Catalysis of the hydrolysis of phosphorylated pyridines by Mg (OH)+: a possible model for enzymic phosphoryl transfer. **Biochemistry**, v. 29, n. 21, p. 5172–5179, 1990.

HOLZ, M. K.; BLENIS, J. Identification of S6 kinase 1 as a novel mammalian target of rapamycin (mTOR)-phosphorylating kinase. **The Journal of Biological Chemistry**, v. 280, n. 28, p. 26089–26093, 15 jul. 2005.

KHAN, M. A. B. et al. Epidemiology of Type 2 Diabetes - Global Burden of Disease and Forecasted Trends. **Journal of Epidemiology and Global Health**, v. 10, n. 1, p. 107–111, mar. 2020.

KIM, D. H. et al. GbetaL, a positive regulator of the rapamycin-sensitive pathway required for the nutrient-sensitive interaction between raptor and mTOR. **Mol Cell**, v. 11, n. 4, p. 895–904, 2003.

KIST, R.; CACERES, R. A. New potential inhibitors of mTOR: a computational investigation integrating molecular docking, virtual screening and molecular dynamics simulation. **Journal of Biomolecular Structure and Dynamics**, v. 35, n. 16, p. 3555–3568, 2016.

KIST, R.; TIMMERS, L. F. S. M.; CACERES, R. A. Searching for potential mTOR inhibitors: Ligand-based drug design, docking and molecular dynamics studies of rapamycin binding site. **Journal of Molecular Graphics and Modelling**, v. 80, p. 251–263, mar. 2018.

KMIECIK, S. et al. Coarse-Grained Protein Models and Their Applications. **Chemical Reviews**, v. 116, n. 14, p. 7898–7936, 27 jul. 2016.

KNIGHT, S. D. et al. Discovery of GSK2126458, a Highly Potent Inhibitor of PI3K and the Mammalian Target of Rapamycin. **ACS Med Chem Lett**, v. 1, n. 1, p. 39–43, 2010.

LAPLANTE, M.; SABATINI, D. M. mTOR signaling at a glance. **J Cell Sci**, v. 122, n. Pt 20, p. 3589–3594, 2009.

LAPLANTE, M.; SABATINI, D. M. mTOR signaling in growth control and disease. **Cell**, v. 149, n. 2, p. 274–293, 2012.

LASKOWSKI, R. A.; SWINDELLS, M. B. LigPlot+: multiple ligand-protein interaction diagrams for drug discovery. **J Chem Inf Model**, v. 51, n. 10, p. 2778–2786, 2011.

LUO, Y. Selectivity assessment of kinase inhibitors: strategies and challenges. **Curr Opin Mol Ther**, v. 7, n. 3, p. 251–255, 2005.

MARTÍNEZ, L.; BORIN, I. A.; SKAT, M. S. Fundamentos de Simulação por Dinâmica Molecular. In: MORGAN, N. H.; COUTINHO, K. (Eds.). . **Métodos de Química Teórica e Modelagem Molecular**. São Paulo: [s.n.]. p. 413–452.

MATTE, A.; TARI, L. W.; DELBAERE, L. T. How do kinases transfer phosphoryl groups? **Structure**, v. 6, n. 4, p. 413–419, 15 abr. 1998.

MUKHERJEE, B. et al. The dual PI3K/mTOR inhibitor NVP-BEZ235 is a potent inhibitor of ATM- and DNA-PKCs-mediated DNA damage responses. **Neoplasia**, v. 14, n. 1, p. 34–43, 2012.

MULLARD, A. First targeted protein degrader hits the clinic. **Nature Reviews Drug Discovery**, v. 18, n. 4, p. 237–239, 6 mar. 2019.

MULLARD, A. Targeted degraders clear first safety hurdles. **Nature Reviews. Drug Discovery**, v. 19, n. 7, p. 435, jul. 2020.

MULLARD, A. Targeted protein degraders crowd into the clinic. **Nature Reviews Drug Discovery**, v. 20, n. 4, p. 247–250, 18 mar. 2021.

NAMBA, A. M.; DA SILVA, V. B.; DA SILVA, C. H. T. P. Dinâmica molecular: teoria e aplicações em planejamento de fármacos. **Eclética Química**, v. 33, n. 4, p. 13–24, 2008.

OZOHANICS, O.; AMBRUS, A. Hydrogen-Deuterium Exchange Mass Spectrometry: A Novel Structural Biology Approach to Structure, Dynamics and Interactions of Proteins and Their Complexes. **Life (Basel, Switzerland)**, v. 10, n. 11, p. E286, 15 nov. 2020.

PEARCE, L. R. et al. Identification of Protor as a novel Rictor-binding component of mTOR complex-2. **The Biochemical Journal**, v. 405, n. 3, p. 513–522, 1 ago. 2007.

PEI, H. et al. Small molecule PROTACs: an emerging technology for targeted therapy in drug discovery. **RSC Advances**, v. 9, n. 30, p. 16967–16976, 29 maio 2019.

PENG, X. et al. Protein–protein interactions: detection, reliability assessment and applications. **Briefings in Bioinformatics**, p. bbw066, 21 jul. 2016.

PETERSON, R. T. et al. FKBP12-rapamycin-associated protein (FRAP) autophosphorylates at serine 2481 under translationally repressive conditions. **The Journal of Biological Chemistry**, v. 275, n. 10, p. 7416–7423, 10 mar. 2000.

PETRYLAK, D. P. et al. First-in-human phase I study of ARV-110, an androgen receptor (AR) PROTAC degrader in patients (pts) with metastatic castrate-resistant prostate cancer (mCRPC) following enzalutamide (ENZ) and/or abiraterone (ABI). **Journal of Clinical Oncology**, v. 38, n. 15_suppl, p. 3500–3500, 20 maio 2020.

PETTERSEN, E. F. et al. UCSF Chimera–a visualization system for exploratory research and analysis. **J Comput Chem**, v. 25, n. 13, p. 1605–1612, 2004.

PETTERSSON, M.; CREWS, C. PROteolysis TArgeting Chimeras (PROTACs) - Past, Present and Future. **Drug discovery today. Technologies**, v. 31, p. 15–27, abr. 2019.

PORTA, C.; PAGLINO, C.; MOSCA, A. Targeting PI3K/Akt/mTOR Signaling in Cancer. **Front Oncol**, v. 4, p. 64, 2014.

QI, S.-M. et al. PROTAC: An Effective Targeted Protein Degradation Strategy for Cancer Therapy. **Frontiers in Pharmacology**, v. 12, p. 1124, 2021.

SANTOS DE OLIVEIRA, F. L. et al. mTOR–mLST8 interaction: hot spot identification through quantum biochemistry calculations. **New Journal of Chemistry**, v. 44, n. 48, p. 20982–20992, 2020.

SANTULLI, G.; TOTARY-JAIN, H. Tailoring mTOR-based therapy: molecular evidence and clinical challenges. **Pharmacogenomics**, v. 14, n. 12, p. 1517–1526, 2013.

SARBASSOV, D. D. et al. Rictor, a novel binding partner of mTOR, defines a rapamycin-insensitive and raptor-independent pathway that regulates the cytoskeleton. **Curr Biol**, v. 14, n. 14, p. 1296–1302, 2004.

SARBASSOV, D. D. et al. Phosphorylation and regulation of Akt/PKB by the rictor-mTOR complex. **Science (New York, N.Y.)**, v. 307, n. 5712, p. 1098–1101, 18 fev. 2005.

SAXTON, R. A.; SABATINI, D. M. mTOR Signaling in Growth, Metabolism, and Disease. **Cell**, v. 168, n. 6, p. 960–976, 9 mar. 2017.

SEHGAL, S. N. Sirolimus: its discovery, biological properties, and mechanism of action. **Transplant Proc**, v. 35, n. 3 Suppl, p. 7S-14S, 2003.

SEKULIĆ, A. et al. A direct linkage between the phosphoinositide 3-kinase-AKT signaling pathway and the mammalian target of rapamycin in mitogen-stimulated and transformed cells. **Cancer Res**, v. 60, n. 13, p. 3504–3513, 2000.

SHIMOBAYASHI, M.; HALL, M. N. Making new contacts: the mTOR network in metabolism and signalling crosstalk. **Nat Rev Mol Cell Biol**, v. 15, n. 3, p. 155–162, 2014.

SHOWKAT, M.; BEIGH, M. A.; ANDRABI, K. I. **mTOR Signaling in Protein Translation Regulation: Implications in Cancer Genesis and Therapeutic Interventions**.

Research article. Disponível em: <https://www.hindawi.com/journals/mbi/2014/686984/>. Acesso em: 12 abr. 2018.

SMITH, H. J.; SIMONS, C. **Enzymes and their inhibitors: drug development**. [s.l.] CRC press, 2004. v. 2

SOLIMAN, G. A. The role of mechanistic target of rapamycin (mTOR) complexes signaling in the immune responses. **Nutrients**, v. 5, n. 6, p. 2231–2257, 2013.

SUN, X. et al. PROTACs: great opportunities for academia and industry. **Signal Transduction and Targeted Therapy**, v. 4, n. 1, p. 1–33, 24 dez. 2019.

SUNG, H. et al. Global Cancer Statistics 2020: GLOBOCAN Estimates of Incidence and Mortality Worldwide for 36 Cancers in 185 Countries. **CA: A Cancer Journal for Clinicians**, v. 71, n. 3, p. 209–249, 2021.

TAO, Z. et al. Steady-state kinetic and inhibition studies of the mammalian target of rapamycin (mTOR) kinase domain and mTOR complexes. **Biochemistry**, v. 49, n. 39, p. 8488–8498, 5 out. 2010.

TEE, A. R.; BLENIS, J. mTOR, translational control and human disease. **Seminars in Cell & Developmental Biology**, v. 16, n. 1, p. 29–37, fev. 2005.

THAIMATTAM, R. et al. Protein kinase inhibitors: structural insights into selectivity. **Curr Pharm Des**, v. 13, n. 27, p. 2751–2765, 2007.

THOREEN, C. C. et al. An ATP-competitive mammalian target of rapamycin inhibitor reveals rapamycin-resistant functions of mTORC1. **J Biol Chem**, v. 284, n. 12, p. 8023–8032, 2009.

VANDER HAAR, E. et al. Insulin signalling to mTOR mediated by the Akt/PKB substrate PRAS40. **Nature Cell Biology**, v. 9, n. 3, p. 316–323, mar. 2007.

WACHECK, V. mTOR pathway inhibitors in cancer therapy: moving past rapamycin. **Pharmacogenomics**, v. 11, n. 9, p. 1189–1191, 2010.

WANG, L. et al. Discovering new mTOR inhibitors for cancer treatment through virtual screening methods and in vitro assays. **Scientific Reports**, v. 6, p. 18987, 2016.

WATANABE, R.; WEI, L.; HUANG, J. mTOR signaling, function, novel inhibitors, and therapeutic targets. **J Nucl Med**, v. 52, n. 4, p. 497–500, 2011.

WORLD HEALTH ORGANIZATION. **Obesity and Overweight**. Disponível em: <https://www.who.int/news-room/fact-sheets/detail/obesity-and-overweight>. Acesso em: 10 mar. 2022.

YANG, H. et al. mTOR kinase structure, mechanism and regulation. **Nature**, v. 497, n. 7448, p. 217–223, 2013.

YUAN, J. et al. PF-04691502, a potent and selective oral inhibitor of PI3K and mTOR kinases with antitumor activity. **Mol Cancer Ther**, v. 10, n. 11, p. 2189–2199, 2011.

ZAROGOULIDIS, P. et al. mTOR pathway: A current, up-to-date mini-review (Review). **Oncol Lett**, v. 8, n. 6, p. 2367–2370, 2014.

ZASK, A.; VERHEIJEN, J. C.; RICHARD, D. J. Recent advances in the discovery of small-molecule ATP competitive mTOR inhibitors: a patent review. **Expert Opin Ther Pat**, v. 21, n. 7, p. 1109–1127, 2011.

ZHAO, Y.; XIONG, X.; SUN, Y. DEPTOR, an mTOR inhibitor, is a physiological substrate of SCF(βTrCP) E3 ubiquitin ligase and regulates survival and autophagy. **Mol Cell**, v. 44, n. 2, p. 304–316, 2011.

ZHENG, Y.; JIANG, Y. mTOR Inhibitors at a Glance. **Mol Cell Pharmacol**, v. 7, n. 2, p. 15–20, 2015.

2 OBJETIVOS

2.1 Objetivo Principal

Aplicar ferramentas *in silico* a fim de compreender a dinâmica do mecanismo molecular de ativação do complexo mTOR-mLst8 para o desenvolvimento de estratégias terapêuticas de controle da via de sinalização.

2.2 Objetivos Específicos

- Modelar estrutura do complexo mTOR-mLst8 para obter um modelo estrutural completo do complexo mTOR-mLst8;
- Realizar simulações por dinâmica molecular com modelos *coarse-grained* para avaliar o comportamento da acoplagem mTOR-mLst8 e o impacto no processo de fosfotransferência;
- Obter o perfil de ligação mTOR-mLst8 para orientar o desenvolvimento de PROTACs.

3 RESULTADOS

3.1 Artigo I

Journal

Molecular Simulation

Title

Understanding the role of mTOR-mLst8 binding through coarse-grained simulation approaches

Running Head

mTOR through CG approaches

Graphical abstract

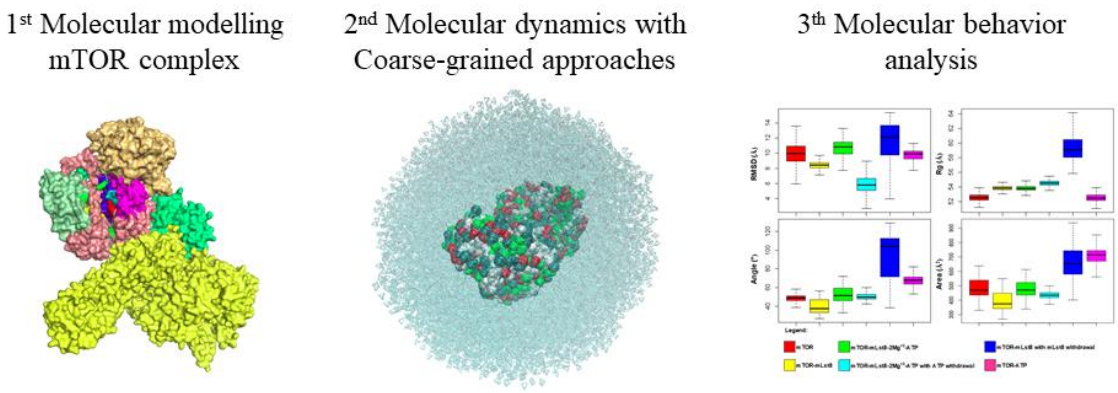

Authors

Roger Kist[a,*], Luis Fernando Saraiva Macedo Timmers[b], Rafael Andrade Caceres[a,c]

[a]Graduate Program in Health Sciences of Federal University of Health Sciences of Porto Alegre – UFCSPA, Porto Alegre City, Brazil.

[b]Graduate Program in Biotechnology, University of Taquari Valley - Univates, Lajeado, RS, Brazil.

[c]Pharmacosciences Department of Federal University of Health Sciences of Porto Alegre – UFCSPA, Porto Alegre City, Brazil.

*Corresponding author. Email: rogerkist@gmail.com. Phone number: +55 51 982079988.

ORCID:

Roger Kist: 0000-0001-7338-2431

Luis Fernando Saraiva Macedo Timmers: 0000-0003-0399-5376
Rafael Andrade Caceres: 0000-0002-7752-975X

Abstract

The kinase called mechanistic Target of Rapamycin (mTOR) belongs to a complex network pathway responsible for many physiological mechanisms, responses to multiple factors and usually is deregulated in various types of diseases. *In vitro* studies support the idea that the binding of mammalian lethal with SEC13 protein 8 (mLst8) subunit on mTOR is necessary to initiate the kinase phosphotransference process. Thus, the mLst8 subunit is important for the regulation of mTOR complex, but its function, especially on catalytic site, needs to be defined. In addition, the contribution of mLst8 to the development and control of pathologies, particularly those in which the mTOR pathways seems deregulated, remains unsolved or with few available data and could be an important step to develop new strategies avoiding the superexpression of this pathway. In our study, we employed coarse-grained molecular dynamics simulation to analyze the behavior of the mTOR catalytic site when the subunit mLst8 is associated or not, providing insights about the importance of mTOR-mLst8 interaction for the kinase mechanism.

Keywords

Mechanistic target of rapamycin; Coarse-grained simulation; mTOR-mLst8 interaction; Catalytic site stabilization

Introduction

The mTOR pathway performs a crucial role in coordinating many physiological mechanisms such as cell growth, division and control. The mTOR is the main kinase of this complex pathway and its control depends of nutrients level, growth factors and the energy status of the cell [1–3]. This atypical kinase is evolutionarily conserved from yeast to mammals and appears in two different functional and structurally complexes – the mTORC1 and mTORC2 complexes that are located in different cell compartments, each containing some common and distinct subunits required for regulation, modulation and catalytic activity of the major enzyme [1–9].

The rapamycin-sensitive mTORC1 contains mTOR, mLst8, Raptor (regulatory protein associated with mTOR) and PRAS40 (proline-rich AKT substrate 40 kDa) [10–13] that regulates cell growth and translation in part by phosphorylating S6K (a ribosomal protein kinase) and the eIF-4E binding protein 1 (4E-BP1) [2,14]. The rapamycin-insensitive mTORC2 contains mTOR, mLst8, Rictor (Rapamycin-insensitive companion of Tor), mSin1 (mammalian stress-activated protein kinase SAPK-interacting protein) and Protor 1/2 (protein observed with Rictor) [2,8,15–19] and regulates the organization of actin cytoskeleton through the phosphorylation of PKCα and Akt kinases [18,20].

Structurally, at mTOR N-terminus domain there is two adjacent HEAT (Huntington, EF3A, ATM, TOR; from residue 17 to residue 1260) domains – the N-terminal HEAT (N-HEAT; from residue 17 to residue 932) and the middle HEAT (M-HEAT; from residue 933 to residue 1260). Following by the FAT (FRAP, ATM, TRRAP; from residue 1261 to residue 2001) domain, and the kinase domain (KD; from residue 2002 to residue 2549) at the C-terminus, which is formed by N-ter (from residue 2002 to residue 2240) and C-ter (from residue 2241 to residue 2549) lobes as others canonical eukaryote protein kinases. In the N-ter lobe, is found the FRB (FKBP12-rapamycin Binding; from residue 2021 to residue 2118). The mLst8 binding element (LBE; from residue 2258 to residue 2296) is located at the C-ter lobe, serving as a binding platform for mLst8. In addition, at the C-terminus of mTOR is situated the FAT C-terminal (FATC; from residue 2519 to residue 2549) domain (**Figure 1**) [6–8,21].

The mLst8 subunit is approximately 40 amino acids residues repeats forming a circular motif. At one end of this motif is a surface that extends to the LBE region of the C-lobe KD. The interaction between mLst8 and LBE enfolds mainly polar residues of LBE with polar/aromatic residues of mLst8, and the interaction contains a large number of hydrogen bonds. This interaction steadies LBE and influences the LBE/FATC/activation-loop, supporting the hypothesis that mLst8 is a crucial subunit for mTOR pathway activation [21,22].

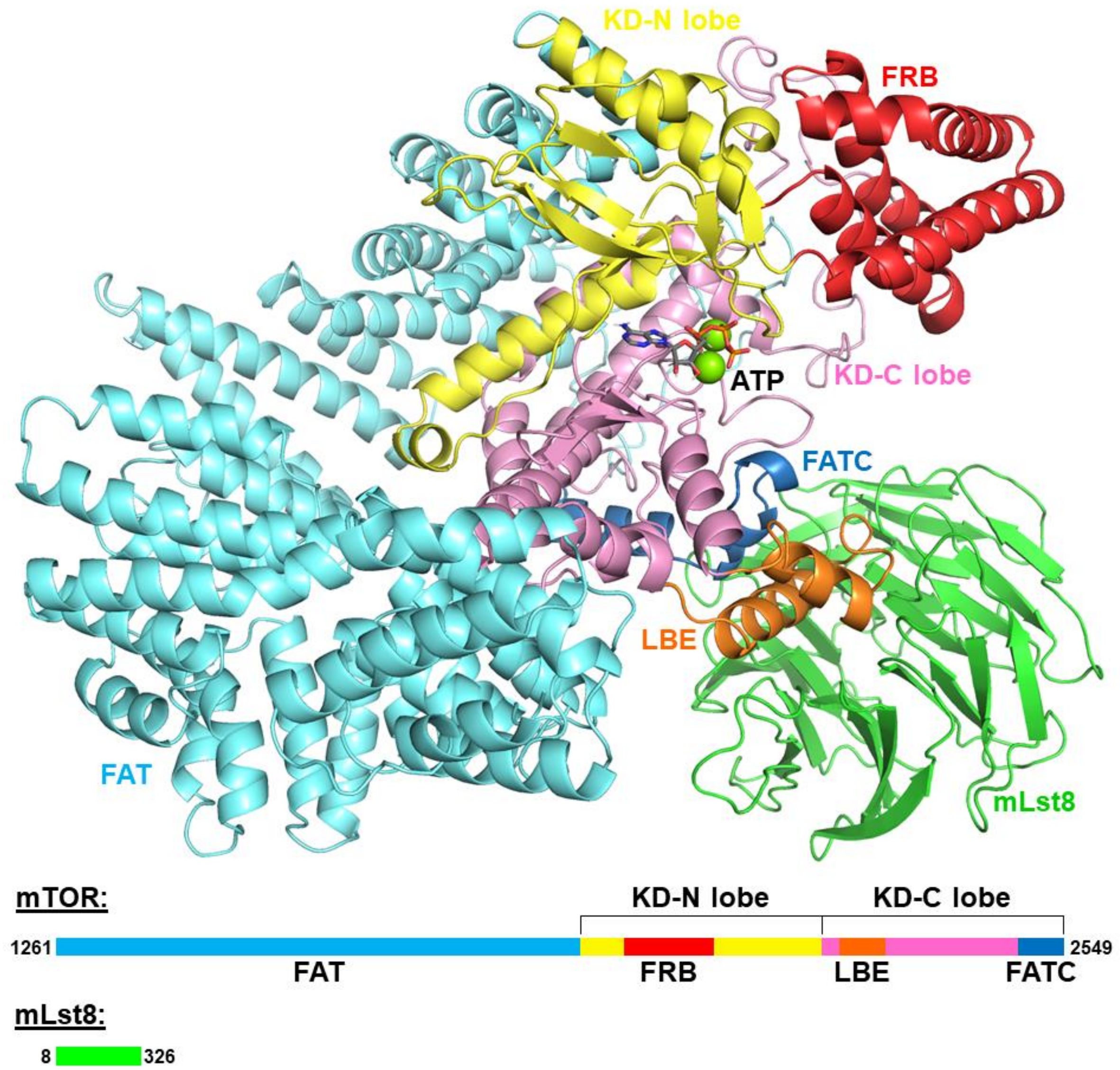

Figure 1. Structure of the mTOR-mLST8-ATP-Mg complex. mTOR is represented as cartoon and colored as indicated in the linear schematic; mLST8 is shown as cartoon and colored in green. The ligands are colored according to CPK scheme, where ATP is sticks and Mg^{2+} ions are spheres. Due to dimension, HEAT domains (from residue 17 to 1260) are not shown in the figure. Figure generated with PyMOL.

The molecular mechanisms regarding the regulation of mTOR activity were elucidated by Yang et al (2013) using a structure of mTOR-mLst8 [21]. The mLst8 is a usual subunit of complexes, mTORC1 and mTORC2, and the association of this subunit is required for mTOR activation. The structure of the mTOR-mLst8 complex demonstrated that mLst8 stabilizes the active site of mTOR, supporting the theory that mLst8 subunit develops an important role in the activity and regulation of this kinase, since embryonic and fibroblast analyzes of mLst8-knockout mice showed that mLst8 is necessary for the formation of the mTOR complex [2,5,21,23,24]. Thus, the mLst8 subunit is important for the normal regulation of both mTOR complexes, but its function, mostly on catalytic site, and how mLst8 binds onto mTOR to perform its activity still unclear. In addition, the contribution of mLst8 to the development and control of pathologies, especially those in which the mTOR pathways are uncontrolled, remains uncharacterized and could be an important step to develop new strategies to regulate this pathway.

Considering the large number of residues of mTOR-mLst8 complex (about 2800 amino acids residues), atomistic approaches become computational expensive. Therefore, we employed coarse-grained molecular dynamics simulation to understand the behavior of mTOR catalytic site when mLst8 is associated or non-associated. Furthermore, based on the computational experiments we suggest hypotheses concerning these binding mechanisms.

Material and methods

Molecular modeling

All experiments were carried out using the Cryo-EM structure of the mTOR-mLst8-Mg-ATP complex (PDB ID 6BCU), and the missing loops (mTOR: Gly1219-Thr1262, Glu1813-Lys1868 and Thr2434-Val2488; mLst8: Gln667-Asn788 and Lys823-Phe933) were built through comparative modeling. The process was performed using Modeller v.9.19 [25,26]. For each sequence was built 1000 models and selected the one with the lowest energy according to DOPE assessment method evaluation. The stereochemical quality of the model was checked using Procheck [27], Verify 3D [28,29], and RAMPAGE [30] softwares.

Coarse-grained (CG) molecular dynamics (MD) simulations

The CG simulations were performed using SIRAH force field [31,32] as follow: (i) Initial coordinates were obtained from the modeled structure and protonated at pH 7.4. (ii) The atomistic structures were converted to CG by an *ad hoc* script from the SIRAH force field. (iii) The CG model was solvated using a prestabilized box of WT4 molecules [33–36]. (iv) Ionic electroneutrality was setted by substituting WT4 molecules by electrolytes Na^+ and Cl^- atoms. The simulation protocol also included (v) energy minimization, (vi) equilibration, and (vii) production phases.

The starting structures (i) mTOR, (ii) mTOR-2Mg^{+2}-ATP, (iii) mTOR-mLst8, (iv) mTOR-mLst8-2Mg^{+2}-ATP, (v) mTOR-mLst8-2Mg^{+2}-ATP with ATP withdrawal and (vi) mTOR-

mLst8-2Mg^{+2}-ATP with mLst8 withdrawal were protonated using pdb2pqr [37], converted to CG and solvated in an octahedral box with a solute-box distance of 2.0 nm. The ionic electroneutrality was setted to 0.15 M of NaCl. All simulations were performed using GROMACS 2016.3 package [38,39] with a time step of 10 fs and updating the neighbor list every 10 steps. Electrostatic interactions were calculated through Particle Mesh Ewald (PME) [40] with a direct cut off of 1.2 nm and a grid spacing of 0.2 nm. The same cut off was used for vdW interactions. Energy minimization was carried out by 1000 interactions of the steepest descent algorithm. The equilibration phase was performed by 5 ns of MD with positional restraints of 1000 kJ/mol.nm^2 applied to all protein beads.
The production phase was performed by 1 µs using NPT ensemble (310.15 K, 1 atm), V-rescale thermostat [41], and Parrinello−Rahman barostat [42].

Data and statistical analysis

Molecular data analysis and graphical plots from root-mean-square deviation (RMSD), radius of gyration (Rg), angle and area of the index of amino acids residues Lys2370−Val2240−Glu2032 from the mTOR catalytic cleft and distance between LBE-mLst8 residues Glu2285-Ser290; Glu2285-Trp272; Met2281-Tyr222 and Met2271-Lys313 were performed through subroutines written in-house Python [43,44] scripts. For these calculations, a CG coordinate file was obtained from the simulation each 1 ns. RMSD was calculated from the original structure of each simulation in order to comparing the structure behavior of the main chain during the simulations and the Rg to identify possible unfolding and monitoring the compactibility of the protein structure [45–47].
The statistical analysis was performed using R Project for Statistical Computing [48], considering normal distribution through the Kolmogorov-Smirnov Test of Normality (p-value > 0.05) and statistical tests with p-value < 0.05 (CI 95 %) were considered significant.

Results

Although there is few studies regarding mTOR-mLst8 interaction, recently de Oliveira et al (2020) shown interesting results about key residues that control the interaction between mTOR and mLst8 and its work open the discussion for the design and probing of new compounds that perform the disruption/modulation of these interactions [49]. For mTOR-mLst8 interaction, the residues with mayor interactions are located in the mTOR

C-lobe, which is known to form the binding site for mLst8 [21]. According to Oliveira et al (2020), the energy analysis revealed some best interactions between pair-to-pair (LBE-mLst8 residues) interactions on mTOR-mLst8 interface residues and we performed the distance analysis from these residues in the crystallographic structure (PDB ID 6BCU): Glu2285-Ser290 (8.6 Å); Glu2285-Trp272 (7.6 Å); Met2281-Tyr222 (8.7 Å) and Met2271-Lys313 (6.7 Å) and considering residues Glu2032-Val2240-Lys2370 as a catalytic cleft angle, this angle is 35.5 ° as shown in the **Figure 2**.

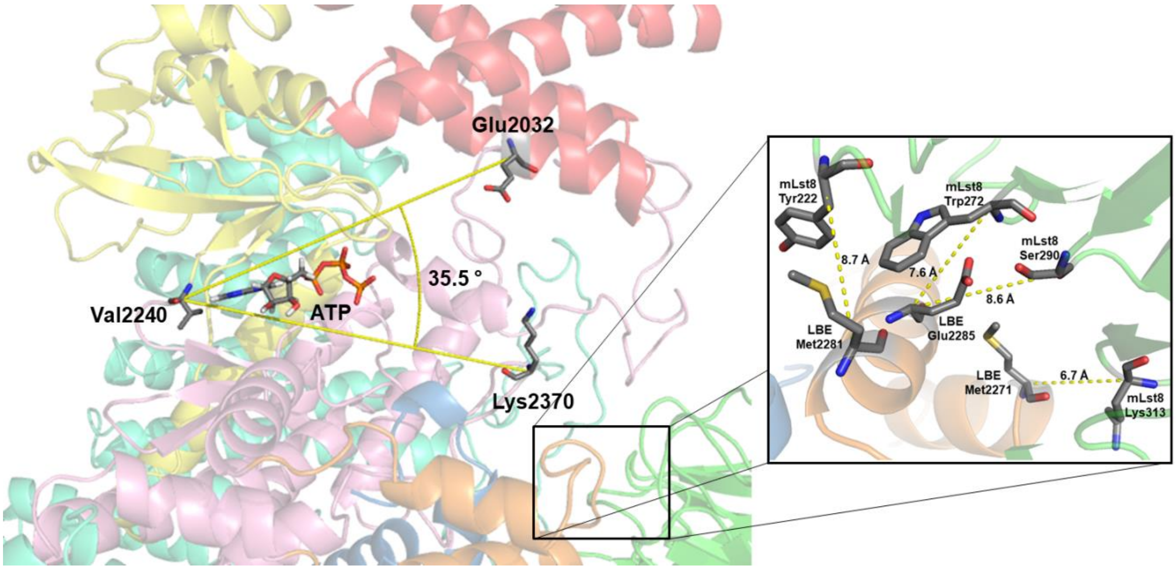

Figure 2. Measurements from catalytic cleft angle and the lowest distances between mLst8 and LBE subunit.

Moreover, our study employed all the mTOR-mLst8 system in a longer CG simulation time that enabled perform the relationship between these interaction residues and the behavior of the catalytic cleft angle (**Figure 3)**. Also, employing the SIRAH backmapping, we extract out structures located at two minima and it was not identified major structural changes in the catalytic site (**Figure 4**). It notes that, for each pair-to-pair interaction, there are two main conformations that enable the control of the catalytic cleft and the angle suffers changes (30 – 50 Å) with a high stabilization of the distance between LBE-mLst8 interactions. These findings purpose that the cleft catalytic opening/closing is an auto-regulated process and depends from the interaction between mTOR-mLst8.

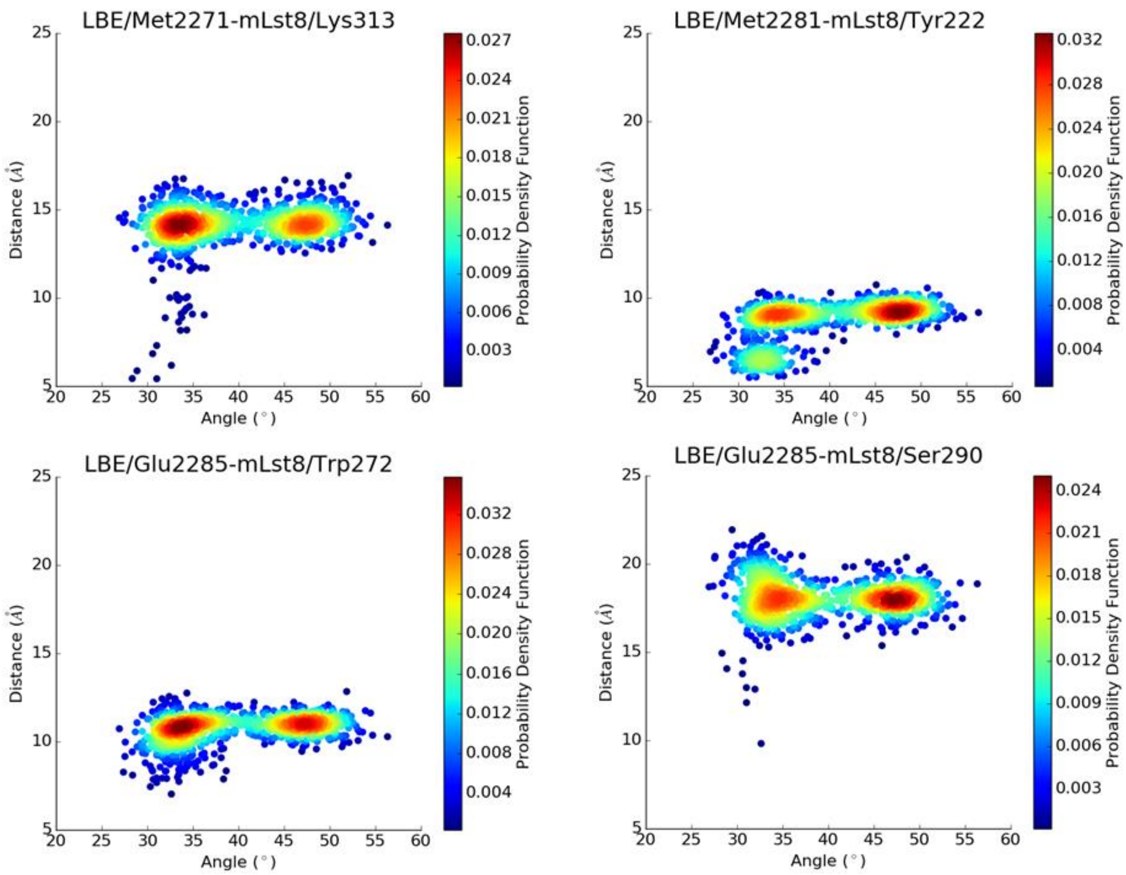

Figure 3. Distance LBE-mLst8 residues *versus* mTOR catalytic cleft angle behavior during the CG simulation.

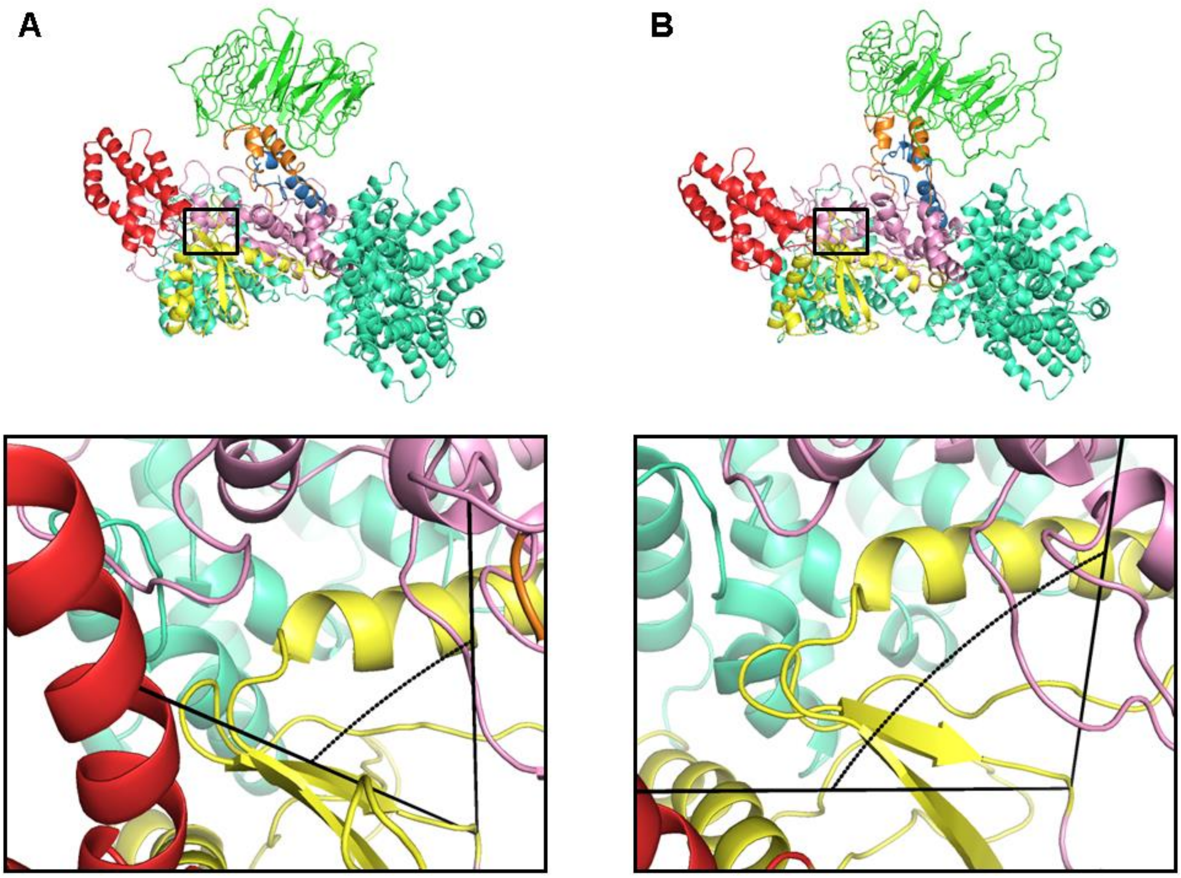

Figure 4. Extracted minima structures from CG simulation employing SIRAH backmapping. (A) Cleft angle of 27.7° and (B) cleft angle of 51.5°.

Considering the catalysis pathway as (i) mTOR → (ii) mTOR- mLst8 binding → (iii) mTOR-mLst8 + $2Mg^{+2}$ + ATP → (iv) mTOR-mLst8-$2Mg^{+2}$-ATP with ATP withdrawal → (v) mTOR-mLst8 with mLst8 withdrawal → (vi) mTOR, the **Figure 5** shows the boxplot of the principal components results obtained from simulation.

The system mTOR-mLst8 shown the smallest values of RMSD, Rg, catalytic cleft angle and area whereas the system mTOR-mLst8 with mLst8 withdrawal shown the opposite, especially the cleft angle values that shown a median of 37.70 Å and variance of 48.38 Å for the system mTOR-mLst8 *versus* median 103.98 Å with variance of 562.66 Å with the mLst8 withdrawn from the system, suggesting that the catalytic cleft is directly affected by the mLst8 subunit.

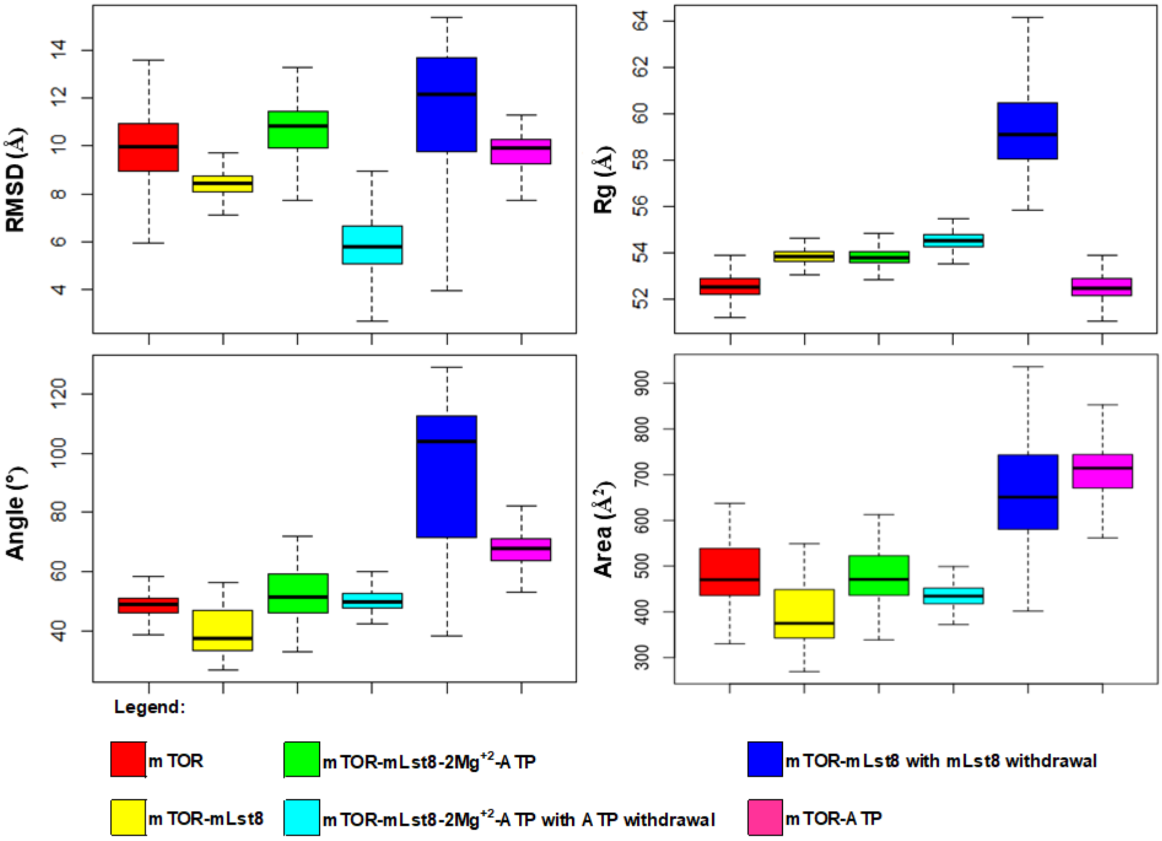

Figure 5. RMSD, Rg, catalytic cleft angle and triangle area boxplots.

Similarly, the cross-data plots (**Figure 6-11)** describe the system destabilization, as a lacking structure organization, especially on catalytic cleft, when mLst8 subunit was not associated to mTOR, following the catalysis pathway. According the statistical analysis, considering that all data did not show normal distribution through the Kolmogorov-Smirnov Test of Normality (*p*-value > 0.05), the Friedman's test with pairwise comparisons using Wilcoxon signed rank test and Bonferroni *p* value adjustment method was employed in order to identify possible differences. The found results were for the RMSD values (chi-squared = 1832.4, p-value < 0.01), Rg values (chi-squared = 4580.2, p-value < 0.01) and cleft angle values (chi-squared = 3784.9, p-value < 0.01). Therefore, there were found statistical differences between the simulated systems, including pairwise comparisons where all the comparisons had p-value < 0.01 that can prove that the kinase behavior is different when mLst8 is binded to the mTOR.

Furthermore, the catalytic cleft suffers remodeling when substrate (ATP) and cofactor (Mg^{+2}) are associated in order to turn the kinase into a catalytically competent configuration (**Figure 10**).

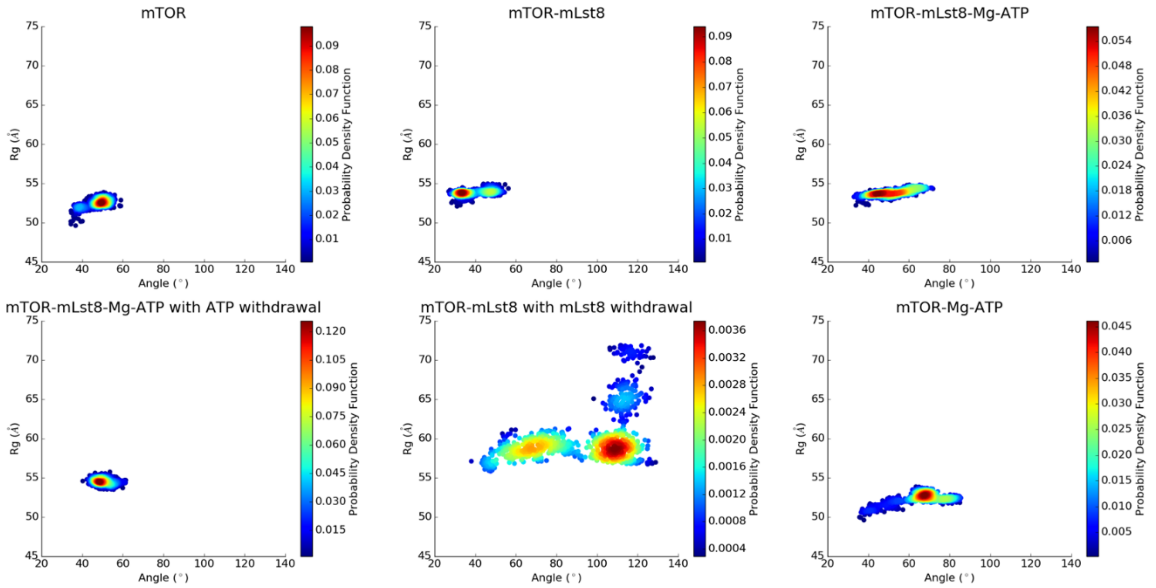

Figure 6. Description of the conformational ensembles regarding the catalytic cleft angle *versus* radius of gyration. The probability density plots highlight the differences in the conformational ensembles according to each simulated system. (A) mTOR, (B) mTOR-mLst8, (C) mTOR-mLst8-Mg-ATP, (D) mTOR-mLst8-Mg-ATP with ATP withdrawal, (E) mTOR-mLst8 with mLst8 withdrawal, (F) mTOR-Mg-ATP.

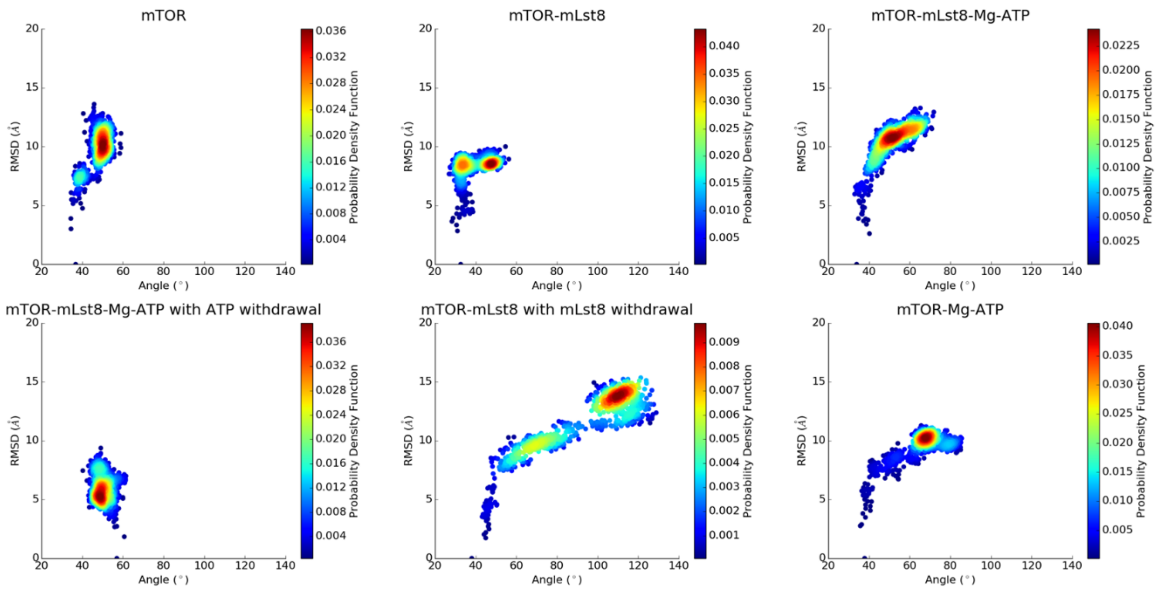

Figure 7. Description of the conformational ensembles regarding the catalytic cleft angle *versus* RMSD. The probability density plots highlight the differences in the

conformational ensembles according to each simulated system. (A) mTOR, (B) mTOR-mLst8, (C) mTOR-mLst8-Mg-ATP, (D) mTOR-mLst8-Mg-ATP with ATP withdrawal, (E) mTOR-mLst8 with mLst8 withdrawal, (F) mTOR-Mg-ATP.

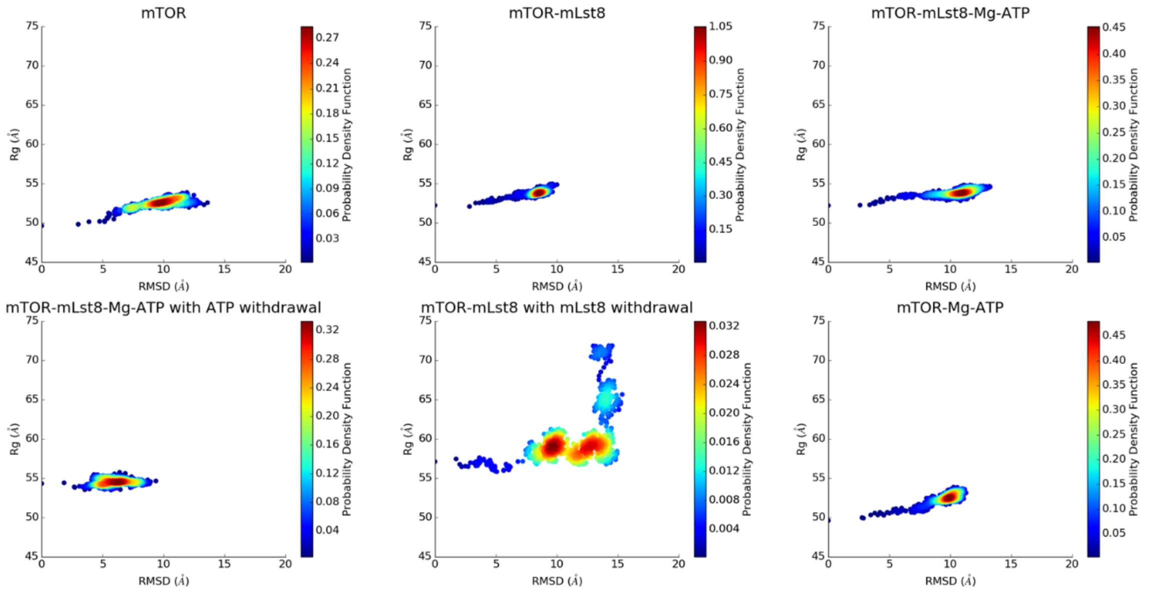

Figure 8. Description of the conformational ensembles regarding the RMSD *versus* radius of gyration. The probability density plots highlight the differences in the conformational ensembles according to each simulated system. (A) mTOR, (B) mTOR-mLst8, (C) mTOR-mLst8-Mg-ATP, (D) mTOR-mLst8-Mg-ATP with ATP withdrawal, (E) mTOR-mLst8 with mLst8 withdrawal, (F) mTOR-Mg-ATP.

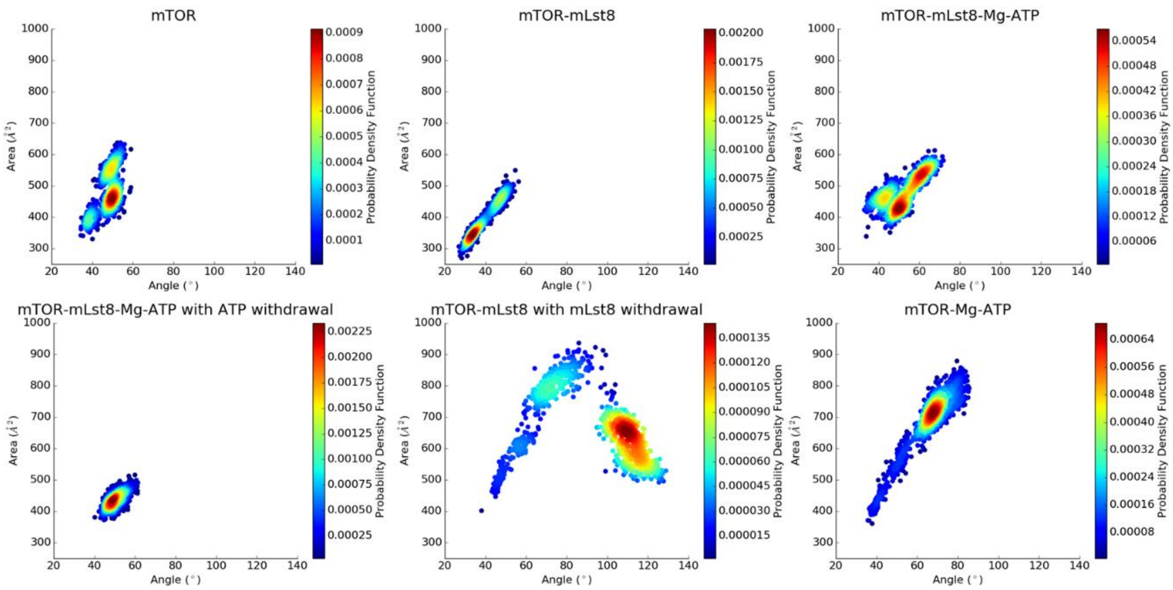

Figure 9. Description of the conformational ensembles regarding the catalytic cleft angle *versus* triangle area. The probability density plots highlight the differences in the

conformational ensembles according to each simulated system. (A) mTOR, (B) mTOR-mLst8, (C) mTOR-mLst8-Mg-ATP, (D) mTOR-mLst8-Mg-ATP with ATP withdrawal, (E) mTOR-mLst8 with mLst8 withdrawal, (F) mTOR-Mg-ATP.

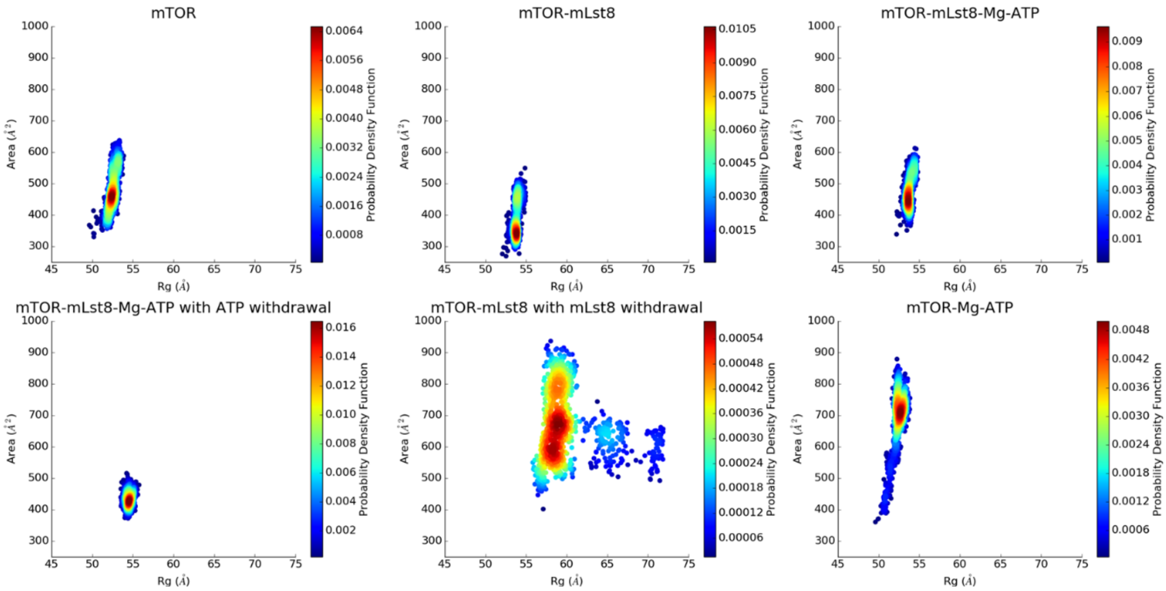

Figure 10. Description of the conformational ensembles regarding the radius of gyration *versus* triangle area. The probability density plots highlight the differences in the conformational ensembles according to each simulated system. (A) mTOR, (B) mTOR-mLst8, (C) mTOR-mLst8-Mg-ATP, (D) mTOR-mLst8-Mg-ATP with ATP withdrawal, (E) mTOR-mLst8 with mLst8 withdrawal, (F) mTOR-Mg-ATP.

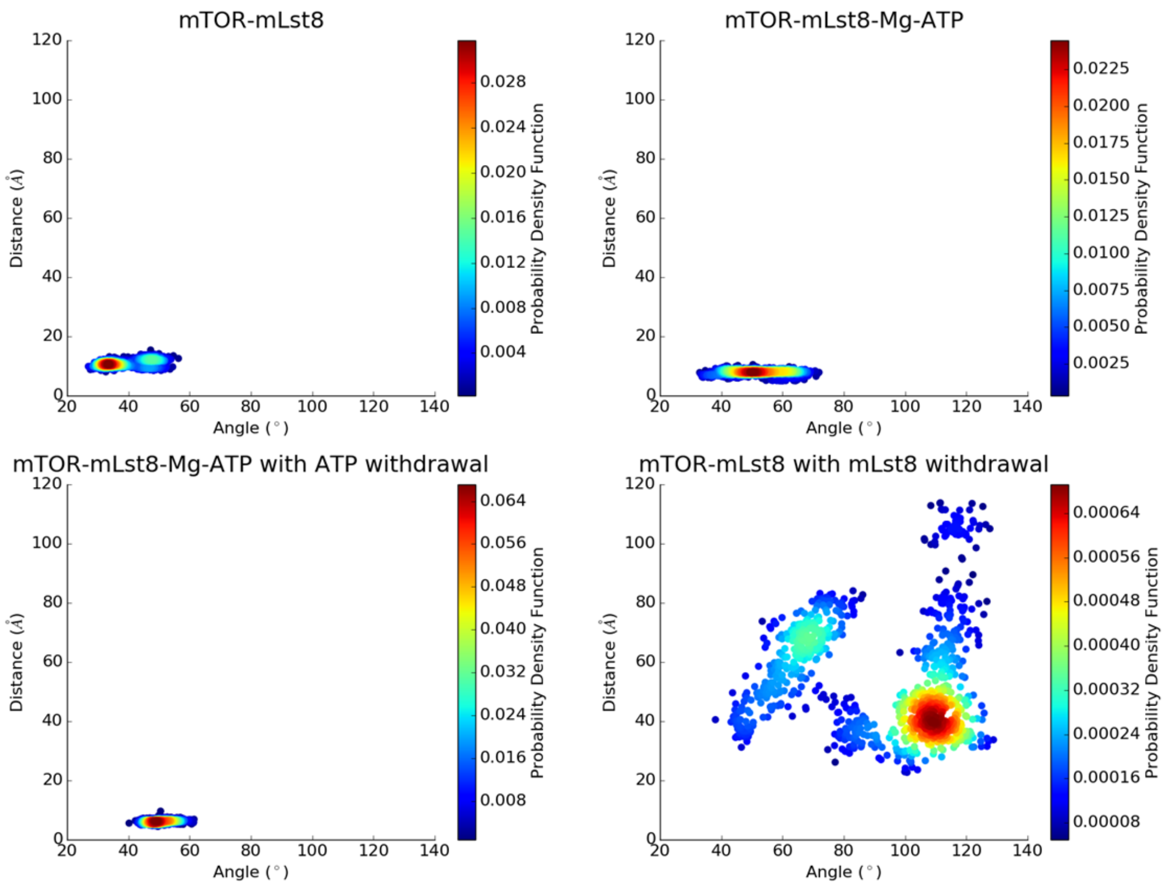

Figure 11. Catalytic cleft angle versus Distance LBE/Glu2285-mLst8/Ser290 plot.

Considering the most populated structures of the simulations based on the catalytic cleft angle (**Figure 12**), it is clear that the presence of mLst8 contributes to the stabilization of the mTOR catalytic site, since the median structures shown the smallest angle on catalytic cleft when the subunit mLst8 was associated. On the other hand, the unbinding of LBE−mLst8 has shown the largest opening of the catalytic cleft with the probability that the phosphotransference mechanism does not occur in this conformation due to the lack of adequate contact between the ATP and catalytic residues.

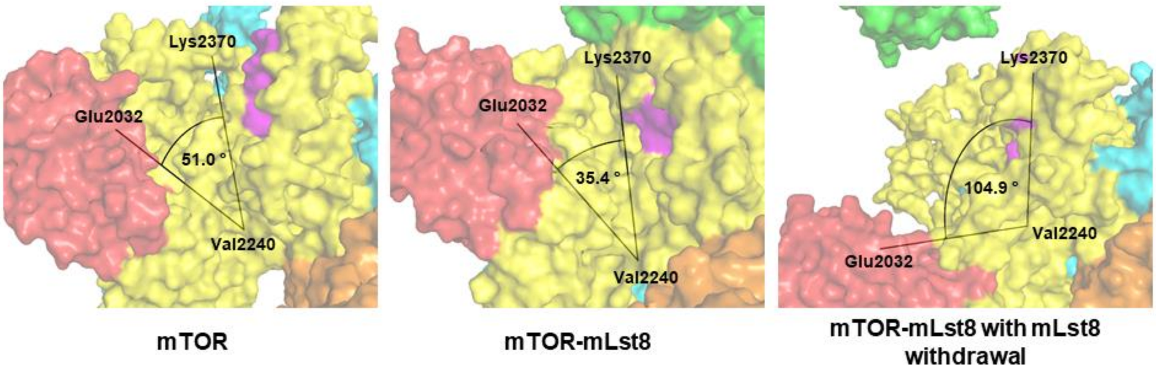

Figure 12. Catalytic cleft angle and catalytic site behavior of median structures.

These results corroborate the hypothesis and previous results, now evidenced through computational approaches, that the binding of mLst8 on mTOR stabilizes the active site of mTOR, favoring phosphotranspherence processes on ATP binding site.

Conclusion

Computational approaches can be very useful to elucidate molecular mechanisms. Employing the SIRAH force field on coarse-grained simulation, we monitored the mTOR catalytic site behavior when mLst8 subunit binds to mTOR and when mLst8 is removed from the complex. These results reinforced the few previous *in vitro* studies where mLst8 is necessary for the formation of the mTOR complex. In addition, these findings could be applied to the development of new strategies to avoid the superexpression of this pathway.

Acknowledgements

We would like to acknowledge the team from Laboratorio de Simulaciones Biomoleculares of Institut Pasteur de Montevideo and Fernando Vieira Lazzarin.

Declarations

Funding: This research did not receive any specific grant from funding agencies in the public, commercial, or not-for-profit sectors.

Conflicts of interest/Competing interests: The authors declare that they have no conflict of interest.

Availability of data and material: N/A

Code availability: N/A

Authors' contributions: N/A

REFERENCES

[1] Conciatori F, Ciuffreda L, Bazzichetto C, et al. mTOR Cross-Talk in Cancer and Potential for Combination Therapy. Cancers [Internet]. 2018 [cited 2019 Sep 1];10. Available from: https://www.ncbi.nlm.nih.gov/pmc/articles/PMC5789373/.

[2] Saxton RA, Sabatini DM. mTOR Signaling in Growth, Metabolism, and Disease. Cell. 2017;168:960–976.

[3] Liu GY, Sabatini DM. mTOR at the nexus of nutrition, growth, ageing and disease. Nat Rev Mol Cell Biol. 2020;21:183–203.

[4] Betz C, Hall MN. Where is mTOR and what is it doing there? J Cell Biol. 2013;203:563–574.

[5] Boutouja F, Stiehm CM, Platta HW. mTOR: A Cellular Regulator Interface in Health and Disease. Cells [Internet]. 2019 [cited 2019 Sep 1];8. Available from: https://www.ncbi.nlm.nih.gov/pmc/articles/PMC6356367/.

[6] Laplante M, Sabatini DM. mTOR signaling at a glance. J Cell Sci. 2009;122:3589–3594.

[7] Laplante M, Sabatini DM. mTOR signaling in growth control and disease. Cell. 2012;149:274–293.

[8] Tafur L, Kefauver J, Loewith R. Structural Insights into TOR Signaling. Genes. 2020;11:885.

[9] Watanabe R, Wei L, Huang J. mTOR signaling, function, novel inhibitors, and therapeutic targets. J Nucl Med. 2011;52:497–500.

[10] Hara K, Maruki Y, Long X, et al. Raptor, a binding partner of target of rapamycin (TOR), mediates TOR action. Cell. 2002;110:177–189.

[11] Kim DH, Sarbassov DD, Ali SM, et al. mTOR interacts with raptor to form a nutrient-sensitive complex that signals to the cell growth machinery. Cell. 2002;110:163–175.

[12] Kim DH, Sarbassov DD, Ali SM, et al. GbetaL, a positive regulator of the rapamycin-sensitive pathway required for the nutrient-sensitive interaction between raptor and mTOR. Mol Cell. 2003;11:895–904.

[13] Vander Haar E, Lee S-I, Bandhakavi S, et al. Insulin signalling to mTOR mediated by the Akt/PKB substrate PRAS40. Nat Cell Biol. 2007;9:316–323.

[14] Tee AR, Blenis J. mTOR, translational control and human disease. Semin Cell Dev Biol. 2005;16:29–37.

[15] Frias MA, Thoreen CC, Jaffe JD, et al. mSin1 is necessary for Akt/PKB phosphorylation, and its isoforms define three distinct mTORC2s. Curr Biol CB. 2006;16:1865–1870.

[16] Jacinto E, Facchinetti V, Liu D, et al. SIN1/MIP1 maintains rictor-mTOR complex integrity and regulates Akt phosphorylation and substrate specificity. Cell. 2006;127:125–137.

[17] Pearce LR, Huang X, Boudeau J, et al. Identification of Protor as a novel Rictor-binding component of mTOR complex-2. Biochem J. 2007;405:513–522.

[18] Sarbassov DD, Ali SM, Kim DH, et al. Rictor, a novel binding partner of mTOR, defines a rapamycin-insensitive and raptor-independent pathway that regulates the cytoskeleton. Curr Biol. 2004;14:1296–1302.

[19] Yang Q, Inoki K, Ikenoue T, et al. Identification of Sin1 as an essential TORC2 component required for complex formation and kinase activity. Genes Dev. 2006;20:2820–2832.

[20] Sarbassov DD, Guertin DA, Ali SM, et al. Phosphorylation and regulation of Akt/PKB by the rictor-mTOR complex. Science. 2005;307:1098–1101.

[21] Yang H, Rudge DG, Koos JD, et al. mTOR kinase structure, mechanism and regulation. Nature. 2013;497:217–223.

[22] Neer EJ, Schmidt CJ, Nambudripad R, et al. The ancient regulatory-protein family of WD-repeat proteins. Nature. 1994;371:297–300.

[23] Guertin DA, Stevens DM, Thoreen CC, et al. Ablation in mice of the mTORC components raptor, rictor, or mLST8 reveals that mTORC2 is required for signaling to Akt-FOXO and PKC alpha but not S6K1. Dev Cell. 2006;11.

[24] Kakumoto K, Ikeda J, Okada M, et al. mLST8 Promotes mTOR-Mediated Tumor Progression. PLoS ONE [Internet]. 2015 [cited 2019 Sep 1];10. Available from: https://www.ncbi.nlm.nih.gov/pmc/articles/PMC4408021/.

[25] Eswar N, Webb B, Marti-Renom MA, et al. Comparative protein structure modeling using Modeller. Curr Protoc Bioinforma. 2006;Chapter 5:Unit 5.6.

[26] Sali A, Blundell TL. Comparative Protein Modelling by Satisfaction of Spatial Restraints. 1993.

[27] Laskowski RA, MacArthur MW, Moss DS, et al. PROCHECK: a program to check the stereochemical quality of protein structures. J Appl Crystallogr. 1993;26:283–291.

[28] Bowie JU, Lüthy R, Eisenberg D. A method to identify protein sequences that fold into a known three-dimensional structure. Science. 1991;253:164–170.

[29] Luthy R, Bowie JU, Eisenberg D. Assessment of protein models with three-dimensional profiles. Nature. 1992;356:83.

[30] Lovell SC, Davis IW, Arendall WB, et al. Structure validation by Calpha geometry: phi,psi and Cbeta deviation. Proteins. 2003;50:437–450.

[31] Darré L, Machado MR, Brandner AF, et al. SIRAH: A Structurally Unbiased Coarse-Grained Force Field for Proteins with Aqueous Solvation and Long-Range Electrostatics. J Chem Theory Comput. 2015;11:723–739.

[32] Machado MR, Pantano S. SIRAH tools: mapping, backmapping and visualization of coarse-grained models. Bioinformatics. 2016;32:1568–1570.

[33] Darré L, Machado MR, Dans PD, et al. Another Coarse Grain Model for Aqueous Solvation: WAT FOUR? J Chem Theory Comput. 2010;6:3793–3807.

[34] Gonzalez HC, Darré L, Pantano S. Transferable Mixing of Atomistic and Coarse-Grained Water Models. J Phys Chem B. 2013;117:14438–14448.

[35] Caceres-Delpiano J, Wang L-P, Essex JW. The Automated Optimisation of a Coarse-Grained Force Field Using Free Energy Data [Internet]. Biophysics; 2020 [cited 2021 May 9]. Available from: http://biorxiv.org/lookup/doi/10.1101/2020.08.13.250233.

[36] Darré L, Tek A, Baaden M, et al. Mixing Atomistic and Coarse Grain Solvation Models for MD Simulations: Let WT4 Handle the Bulk. J Chem Theory Comput. 2012;8:3880–3894.

[37] Dolinsky TJ, Nielsen JE, McCammon JA, et al. PDB2PQR: an automated pipeline for the setup of Poisson-Boltzmann electrostatics calculations. Nucleic Acids Res. 2004;32:W665-667.

[38] Abraham MJ, Murtola T, Schulz R, et al. Gromacs: High performance molecular simulations through multi-level parallelism from laptops to supercomputers. SoftwareX. 2015;1–2.

[39] Van Der Spoel D, Lindahl E, Hess B, et al. GROMACS: fast, flexible, and free. J Comput Chem. 2005;26:1701–1718.

[40] Darden T, York D, Pedersen L. Particle mesh Ewald: An N· log (N) method for Ewald sums in large systems. J Chem Phys. 1993;98:10089–10092.

[41] Bussi G, Donadio D, Parrinello M. Canonical sampling through velocity rescaling. J Chem Phys. 2007;126:014101.

[42] Parrinello M, Rahman A. Polymorphic transitions in single crystals: A new molecular dynamics method. J Appl Phys. 1981;52:7182–7190.

[43] Kagami LP, das Neves GM, Timmers LFSM, et al. Geo-Measures: A PyMOL plugin for protein structure ensembles analysis. Comput Biol Chem. 2020;87:107322.

[44] Van Rossum G, Drake Jr. FL. Python reference manual. Amsterdam: Centrum voor Wiskunde en Informatica.; 1995.

[45] Maiorov VN, Crippen GM. Significance of root-mean-square deviation in comparing three-dimensional structures of globular proteins. J Mol Biol. 1994;235:625–634.

[46] Kufareva I, Abagyan R. Methods of Protein Structure Comparison. In: Orry AJW, Abagyan R, editors. Homol Model [Internet]. Totowa, NJ: Humana Press; 2011 [cited 2021 May 22]. p. 231–257. Available from: http://link.springer.com/10.1007/978-1-61779-588-6_10.

[47] Lobanov MYu, Bogatyreva NS, Galzitskaya OV. Radius of gyration as an indicator of protein structure compactness. Mol Biol. 2008;42:623–628.

[48] Team RC. R: A language and environment for statistical computing. R Foundation for Statistical Computing, Vienna, Austria.[WWW document]. URL Httpwww R-Proj OrgAccessed Dec 24 2013. 2013;

[49] Santos de Oliveira FL, Vieira Carletti J, Azevedo FFN, et al. mTOR–mLST8 interaction: hot spot identification through quantum biochemistry calculations. New J Chem. 2020;44:20982–20992.

3.2 Artigo II

Journal

Journal of Biomolecular Structure and Dynamics

Title

The mTOR-mLst8 binding profile through molecular simulation, free-energy calculation, per-residue decomposition and hydrogen bonds identification

Running head

Understanding mTOR-mLst8 binding profile through *in silico* approaches as tool to control the pathway overexpression

Graphical abstract

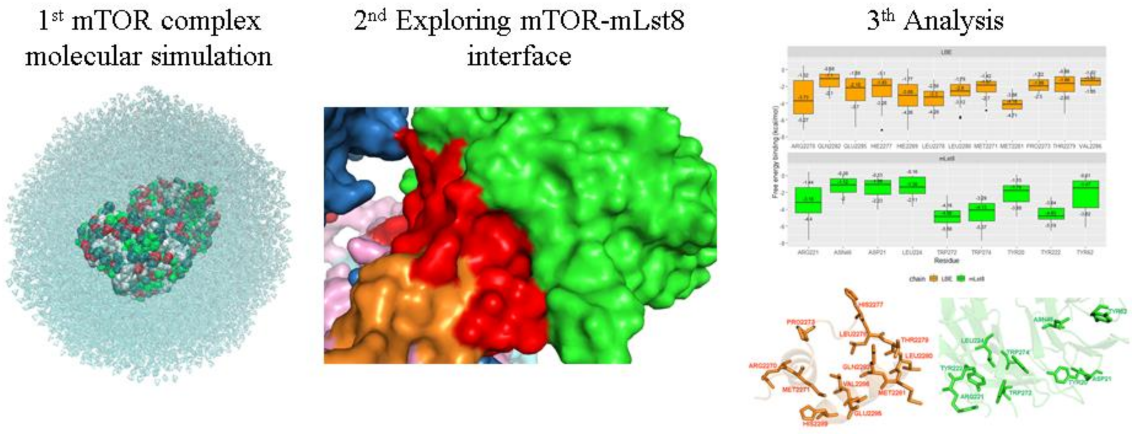

Authors

Roger Kist[a,*], Luis Fernando Saraiva Macedo Timmers[b], Rafael Andrade Caceres[a,c]

[a]Graduate Program in Health Sciences of Federal University of Health Sciences of Porto Alegre – UFCSPA, Porto Alegre City, Brazil.

[b]Graduate Program in Biotechnology, University of Taquari Valley - Univates, Lajeado, RS, Brazil.

[c]Pharmacosciences Department of Federal University of Health Sciences of Porto Alegre – UFCSPA, Porto Alegre City, Brazil.

*Corresponding author. Email: rogerkist@gmail.com. Phone number: +55 51 982079988.

ORCID:

Roger Kist: 0000-0001-7338-2431

Luis Fernando Saraiva Macedo Timmers: 0000-0003-0399-5376
Rafael Andrade Caceres: 0000-0002-7752-975X

Abstract

The mechanistic Target of Rapamycin (mTOR) kinase is the main enzyme from the complex pathway important for many physiological mechanisms and its deregulation is present in various types of diseases. *In silico* and *in vitro* studies reinforce the hypothesis that the entire phosphotransference process occurs after the fundamental binding of mammalian lethal with SEC13 protein 8 (mLst8) subunit on mTOR. However, the characterization of the mTOR-mLst8 binding interface is still lacking in specific studies that aim to identify important residues and their characteristics. In order to obtain insights into mTOR-mLst8 interface at molecular level, molecular dynamic simulation, MM/GBSA approaches, free energy binding calculation and hydrogen bonds evaluation with statistical analysis were employed. In addition, per-residue decomposition of these energies led to the identification of key amino acids and interactions contributing to the differential binding of mTOR-mLst8. Our results indicated that mTOR residues ARG2270, HIS2289, LEU2278 and MET2281 and mLst8 residues ARG221, TRP272, TRP274 and TYR222 were essentials in interaction activity, contributing as binding energy much as hydrogen bonds. Our results would aid in the development of new strategies to control this pathway, disrupting the mTOR-mLst8 binding and avoiding its overexpression.

Keywords

Mechanistic target of rapamycin; Coarse-grained simulation; mTOR-mLst8 interaction; Free-energy calculations; Per-residue decomposition

Introduction

Proteins are the principal functional components of biological systems and they commonly perform interactions with others macromolecules in order to achieve your functions. The protein–protein interactions (PPIs) are the main key to understanding the role of these complexes systems in the execution of many biological processes. Considering the experimental limitations due to the complexes pathways to find all interactions in a proteome, computational prediction of PPI has become an important tool in proteomics research [1–5].

In this background, the mTOR pathway is a complex network constituted by a large number of proteins and independent subunits that work together for regulation, modulation and catalytic activity of the major enzyme, the mTOR [6–9]. The mTOR occurs in two multicomponent kinase complexes, mTORC1 and mTORC2, which are structurally similar but functionally different and both signaling pathways are not independent [6]. For example, for mTORC1, the main enzyme mTOR is linked to the subunits RPTOR (regulatory protein associated with mTOR) and PRAS40 (proline-rich AKT substrate 40 kDa). For mTORC2, the mTOR is linked to RICTOR (Rapamycin-insensitive companion of Tor), mSin1 (mammalian stress-activated protein kinase SAPK-interacting protein) and PROTOR 1/2 (protein observed with Rictor) [10–14].

However, there are two subunits common to both complexes: the DEPTOR (DEP-domain containing mTOR-interacting protein) and an essential subunit that performs the first binding with mTOR in order to turn the kinase active and able for the phosphotransference process – the mLst8 (mammalian lethal with SEC13 protein 8) [15–18].

Regarding the mTOR, structurally at mTOR N-terminus domain there is an adjacent HEAT (Huntington, EF3A, ATM, TOR; from residue 17 to residue 1260) domain, following by the FAT (FRAP, ATM, TRRAP; from residue 1261 to residue 2001) domain, and the kinase domain (KD; from residue 2002 to residue 2549) at the C-terminus, that is formed by N-ter (from residue 2002 to residue 2240) and C-ter (from residue 2241 to residue 2549) lobes as others canonical eukaryote protein kinases. In the N-ter lobe, is found the FRB (FKBP12-rapamycin Binding; from residue 2021 to residue 2118). The mLst8 binding element (LBE; from residue 2258 to residue 2296) is located at the C-ter lobe, serving as a binding platform for mLst8. In addition, at the C-terminus of mTOR is situated the FAT C-terminal (FATC; from residue 2519 to residue 2549) domain. About mLst8, it is formed around 40 amino acids residues repeats forming a circular motif. At one end of this motif is a surface that extends to the LBE region of the C-lobe KD (**Figure 1**) [8,19,20].

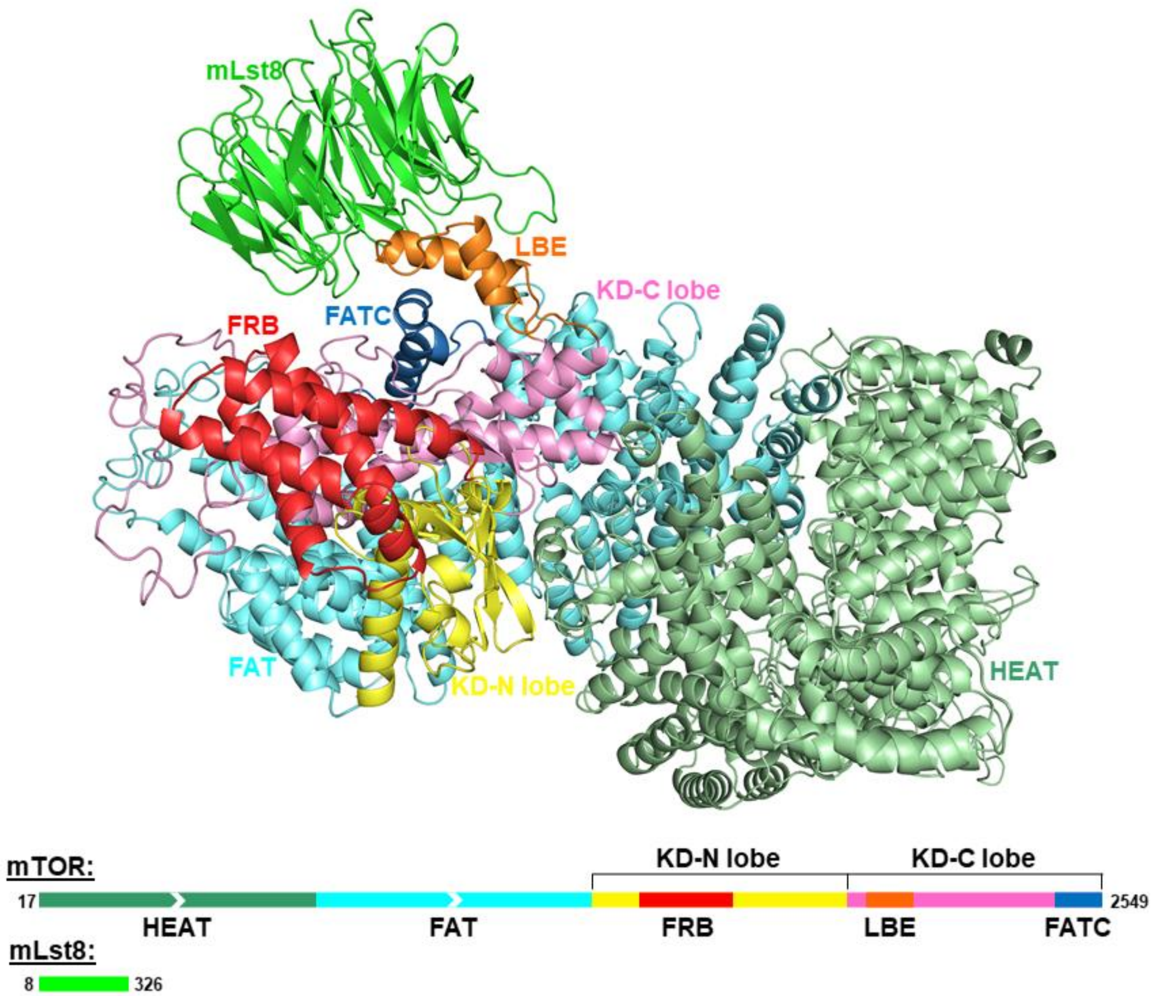

Figure 1. Linear schematic and structure of the mTOR-mLst8 complex. Figure generated with PyMOL.

The interaction between mLst8 and LBE enfolds mainly polar residues of LBE with polar/aromatic residues of mLst8, and the interaction contains a large number of hydrogen bonds. This interaction steadies LBE and influences the LBE/FATC/activation-loop, supporting the hypothesis that mLst8 is a crucial subunit for mTOR pathway activation [19,21].

The abnormal activation of the mTORCs is considered as a key feature of many metabolic disorders such as cancer, diabetes, obesity and neurodegenerative diseases due to mutations, amplification or overexpression of the components of mTOR complexes and mutations or loss of negative regulators of mTOR [9,18,22,23].

In this way, some studies have shown that the K63 linkage polyubiquitination of mLst8, supported by TRAF2, regulates the homeostasis of mTORC1 formation and activation. Especially when the K63 linkage polyubiquitination of mLst8 disrupts its interaction with the mTORC2 component Sin1 to promote mTORC1 formation. Also, the deubiquitinating enzyme OTUD7B was described to help the formation of mTORC2 by removing the polyubiquitin chain on mLst8 and then promoting the interaction between mLst8 and Sin1. Accordingly, the complex dynamic assembly and activation of mTORC1 and mTORC2 are dependent on the ubiquitination of mLst8, further demonstrating the importance of ubiquitination in the mTOR signaling pathway [24,25].

Considering that LBE-mLst8 binding is crucial for activation and regulation of the main kinase activity, that the complex behavior regarding the balance between mTORC1 and mTORC2 and the large amount of residues of mTOR-mLst8 complex, we employed a large coarse-grained molecular dynamic simulation to understand the characteristics of LBE-mLst8 interface in order to describe the free binding energy (FBE) between the subunits and perform per-residue decomposition of these energies led to the identification of crucial amino acids and interactions contributing to the LBE-mLsT8 interaction and to provide knowledge about the residues that perform these interactions and to promote others studies, for example, the creation of proteolysis targeting chimeric (PROTACs) technology [26,27] that enable the degradation via proteasome of mLst8 and enable the inactivation of the mTOR pathway.

Material and methods

Molecular modeling

The Cryo-EM structure of the mTOR-mLst8-Mg-ATP complex (PDB ID 6BCU) was employed to perform all the experiments and the missing loops (mTOR: GLY1219–THR1262, GLU1813–LYS1868 and THR2434–VAL2488; mLst8: GLN667–ASN788 and LYS823–PHE933) were built through comparative modeling using Modeller v.9.19 [28,29].

Coarse-grained (CG) molecular dynamics (MD) simulation

The CG simulation was performed using SIRAH force field [30,31] as follow: (i) Initial coordinates were obtained from the modeled structure and protonated at pH 7.4. (ii) The atomistic structures were converted to CG by an *ad hoc* script from the SIRAH force field. (iii) The CG model was solvated using a prestabilized box of WT4 molecules [32–35]. (iv) Ionic electroneutrality was set by substituting WT4 molecules by electrolytes Na^+ and Cl^- atoms. The simulation protocol also included (v) energy minimization, (vi) equilibration, and (vii) production phases.

The initial structure mTOR-mLst8 was protonated using pdb2pqr [36], converted to CG and solvated in an octahedral box with a solute-box distance of 2.0 nm. The ionic electroneutrality was set to 0.15 M of NaCl. All simulations were performed using GROMACS 2016.3 package [37,38] with a time step of 10 fs and updating the neighbor list every 10 steps. Electrostatic interactions were calculated through Particle Mesh Ewald (PME) [39] with a direct cut off of 1.2 nm and a grid spacing of 0.2 nm. The same cut off was used for vdW interactions. Energy minimization was carried out by 1000 interactions of the steepest descent algorithm. The equilibration phase was performed by 5 ns of MD with positional restraints of 1000 kJ/mol.nm^2 applied to all protein beads. The production phase was performed by 1 μs in order to obtain a satisfactory sampling of the behavior of the mTOR-mLst8 complex, using NPT ensemble (310.15 K, 1 atm), V-rescale thermostat [40] and Parrinello−Rahman barostat [41].

Data and statistical analysis

As shown in **Figure 2**, according our previous catalytic cleft study [17], molecular data analysis and graphical plots from angle of the index of amino acids residues LYS2370−VAL2240−GLU2032 from the mTOR catalytic cleft and distance between LBE-mLst8 residues GLU2285–SER290; GLU2285–TRP272; MET2281–TYR222 and MET2271–LYS313 were performed through subroutines written in-house Python [42,43] scripts. For these calculations, a CG coordinate file was obtained from the simulation each 1 ns.

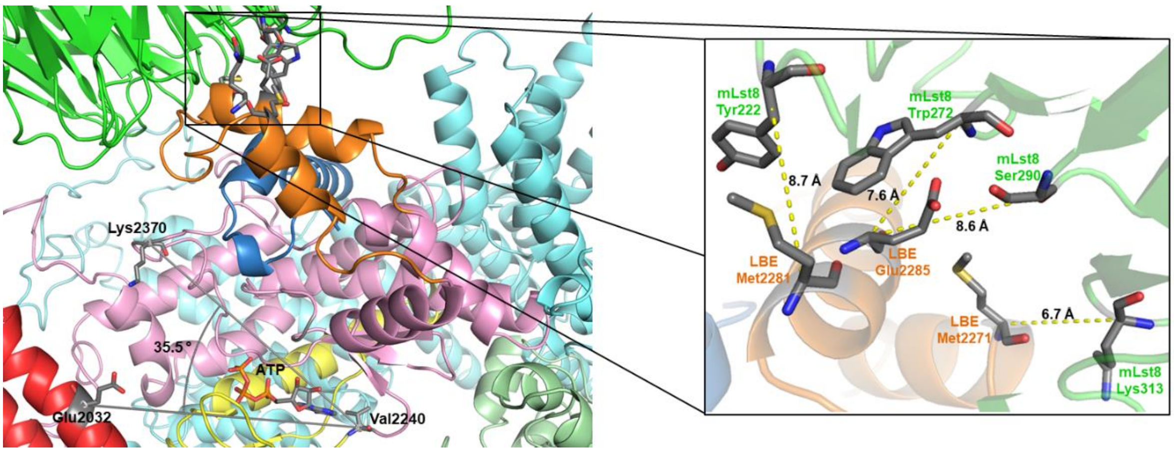

Figure 2. Measurements from catalytic cleft angle and the lowest distances between LBE and mLst8 subunit.

Fifty selected simulated systems plus the crystallographic structure from mTOR-mLst8 had the FBE calculated through molecular mechanics energies combined with generalized Born and surface area continuum solvation (MM/GBSA) method using the platform HawkDock [44] in triplicate. The total FBE are decomposition from van der Waals, electrostatics, Generalized Born and surface area interactions energies from each residue.

For hydrogen bonds analysis, we employed the Hydrogen Bonds Computing Server (HBCS) [45] that uses the program Reduce [46] in order to add hydrogen atoms if are not available in this structure [47].

The statistical analysis was performed using R Project for Statistical Computing [48], considering normal distribution through the Shapiro-Wilk test of normality [49] (p-value > 0.05) and statistical tests with p-value < 0.05 (CI 95 %) were considered significant.

Results

Employing a graphical plot of the probability density function (**Figure 3**), that draw the angle measurement of the index of amino acids residues LYS2370−VAL2240−GLU2032 from the mTOR catalytic cleft *versus* the distance between LBE-mLst8 residues GLU2285–SER290; GLU2285–TRP272; MET2281–TYR222 and MET2271–LYS313 retrieved from performed coarse-grained molecular dynamics, we selected fifty systems (pdb file) (**Table 1**) based on the limits (peripheral points, in blue color) and central (from green to red color) values to compute the FBE. The descriptive analysis from the systems shown that the cleft angle presented average 36.97° (SD ± 6.85°), median 34.45° (min 26.94° – max 51.53°) and distance with average 13.07 Å (SD ± 3.77 Å), median 13.95 Å (min 5.42 Å – max 19.01 Å).

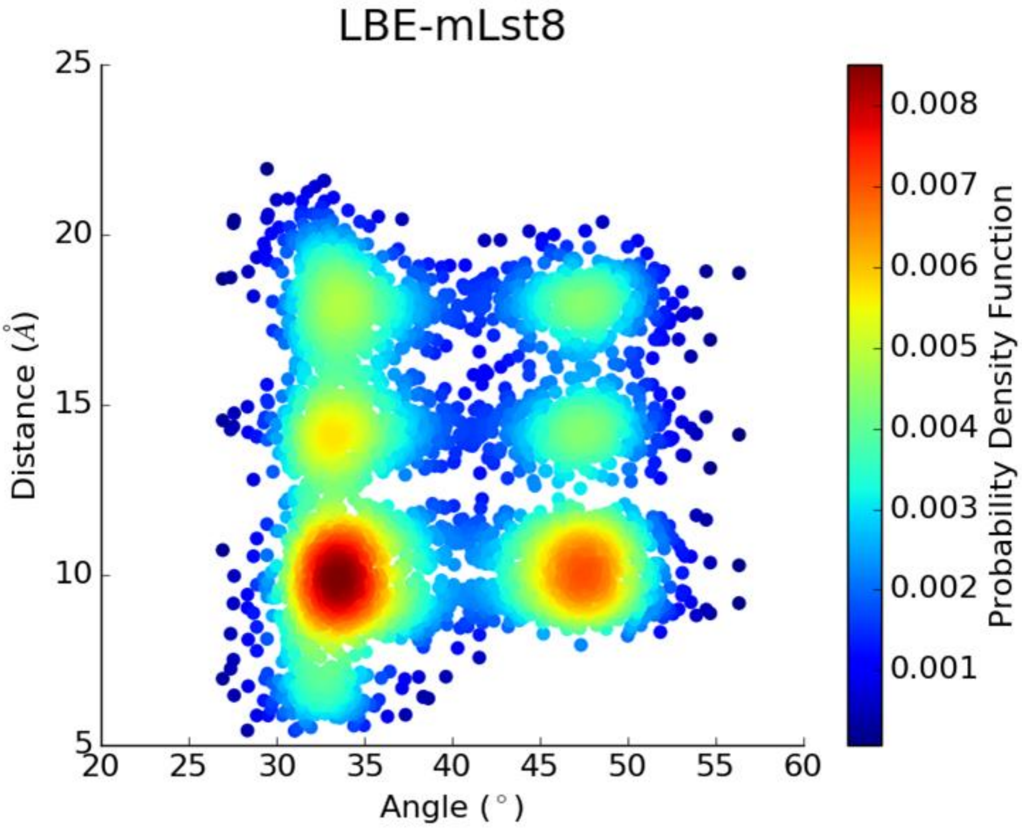

Figure 3. Graphical plot from the angle behavior of the index of amino acids residues LYS2370−VAL2240−GLU2032 from the mTOR catalytic cleft and the distance between LBE-mLst8 residues GLU2285–SER290; GLU2285–TRP272; MET2281–TYR222 and MET2271–LYS313 fetched from performed coarse-grained molecular dynamics.

Time (ns)	Contact	Angle (°)	Distance (Å)	Time (ns)	Contact	Angle (°)	Distance (Å)
1	LBE/2271 - mLst8/313	32.64	6.18	126	LBE/2271 - mLst8/313	31.65	13.44
2	LBE/2271 - mLst8/313	31.04	5.42	140	LBE/2271 - mLst8/313	31.29	14.98
3	LBE/2271 - mLst8/313	30.59	6.84	146	LBE/2271 - mLst8/313	34.78	12.73
4	LBE/2271 - mLst8/313	28.35	5.43	148	LBE/2271 - mLst8/313	34.41	12.90
5	LBE/2271 - mLst8/313	28.88	5.87	151	LBE/2285 - mLst8/272	31.42	10.78
7	LBE/2271 - mLst8/313	31.03	7.30	167	LBE/2285 - mLst8/290	31.01	18.39
8	LBE/2271 - mLst8/313	33.47	11.78	177	LBE/2271 - mLst8/313	26.94	14.54
10	LBE/2271 - mLst8/313	32.47	10.01	222	LBE/2285 - mLst8/272	32.20	11.08
11	LBE/2271 - mLst8/313	33.24	9.98	464	LBE/2281 - mLst8/222	32.79	9.10
14	LBE/2271 - mLst8/313	35.17	11.79	515	LBE/2281 - mLst8/222	36.37	8.92
15	LBE/2271 - mLst8/313	36.32	14.55	558	LBE/2285 - mLst8/272	37.78	11.48
22	LBE/2271 - mLst8/313	37.15	15.69	593	LBE/2271 - mLst8/313	41.07	13.87
23	LBE/2271 - mLst8/313	34.49	14.52	689	LBE/2285 - mLst8/290	47.65	17.92
24	LBE/2271 - mLst8/313	33.89	14.43	690	LBE/2285 - mLst8/290	48.78	17.61

31	LBE/2271 - mLst8/313	33.22	15.69	707	LBE/2285 - mLst8/290	51.53	19.01
32	LBE/2271 - mLst8/313	38.36	14.02	719	LBE/2285 - mLst8/290	46.98	17.47
35	LBE/2271 - mLst8/313	35.58	15.84	725	LBE/2285 - mLst8/290	48.03	17.03
40	LBE/2271 - mLst8/313	34.68	14.59	806	LBE/2281 - mLst8/222	49.81	8.99
41	LBE/2271 - mLst8/313	32.76	15.81	868	LBE/2281 - mLst8/222	43.62	9.62
45	LBE/2271 - mLst8/313	30.51	14.81	874	LBE/2281 - mLst8/222	50.38	9.21
46	LBE/2271 - mLst8/313	32.62	14.92	985	LBE/2285 - mLst8/290	47.37	17.89
47	LBE/2271 - mLst8/313	31.62	13.63	987	LBE/2285 - mLst8/290	44.34	17.28
70	LBE/2271 - mLst8/313	34.59	12.60	992	LBE/2285 - mLst8/290	46.44	17.05
94	LBE/2271 - mLst8/313	33.21	10.18	995	LBE/2285 - mLst8/290	46.69	17.95
119	LBE/2271 - mLst8/313	31.80	14.18	1000	LBE/2285 - mLst8/290	47.59	18.23

Table 1. The features from the fifty systems retrieved from CG simulations.

After HawkDock submission, regarding the FBE results from the 51 retrieved systems, the Shapiro-Wilk normality test revealed that all data generated did not show a Gaussian distribution (*p*-value < 0.05). The Spearman correlation [50] between the FBE residues from the systems revealed ρ (rho) coefficient from 0.68 to 0.92 with *p-value* < 0.05. Employing Friedman's test [51–54] with Nemenyi post-hoc test [55], when the systems and the residues FBE were compared between themselves, both of them comparisons did not show significant difference (*p*-value > 0.05) and, therefore, all the systems and residues presented similar FBE characteristics and the simulation was well sampled. The descriptive analysis from the systems shown that total FBE presented average -64.54 kcal/mol (SD ± 11.62 kcal/mol), median -63.02 kcal/mol (min -99.13 kcal/mol – max -42.98 kcal/mol).

Considering the features of the amino acids side chain as polarity (polar residues: CYS, HIS, ASN, GLN, SER, THR, TYR and TRP; nonpolar residues: ALA, PHE, GLY, ILE, LEU, MET, PRO and VAL; charged residues: ASP, GLU, LYS and ARG) [56,57] and net charge at pH 7.4 (neutral residues: ALA, ASN, CYS, GLN, PHE, GLY, HIS, ILE, LEU, MET, PRO, SER, THR, TRP, TYR and VAL; positive residues: ARG and LYS; negative residues: ASP and GLU) [57], in the **Figure 4** is shown these characteristics from the main residues in the interface LBE-mLst8 and we concluded that 93.35% of FBE is related to the interaction between these 68 residues. Therefore, the residues from LBE subunit have nonpolar and neutral features, meanwhile, the fraction mLst8 has charged/polar and neutral/positive characteristic.

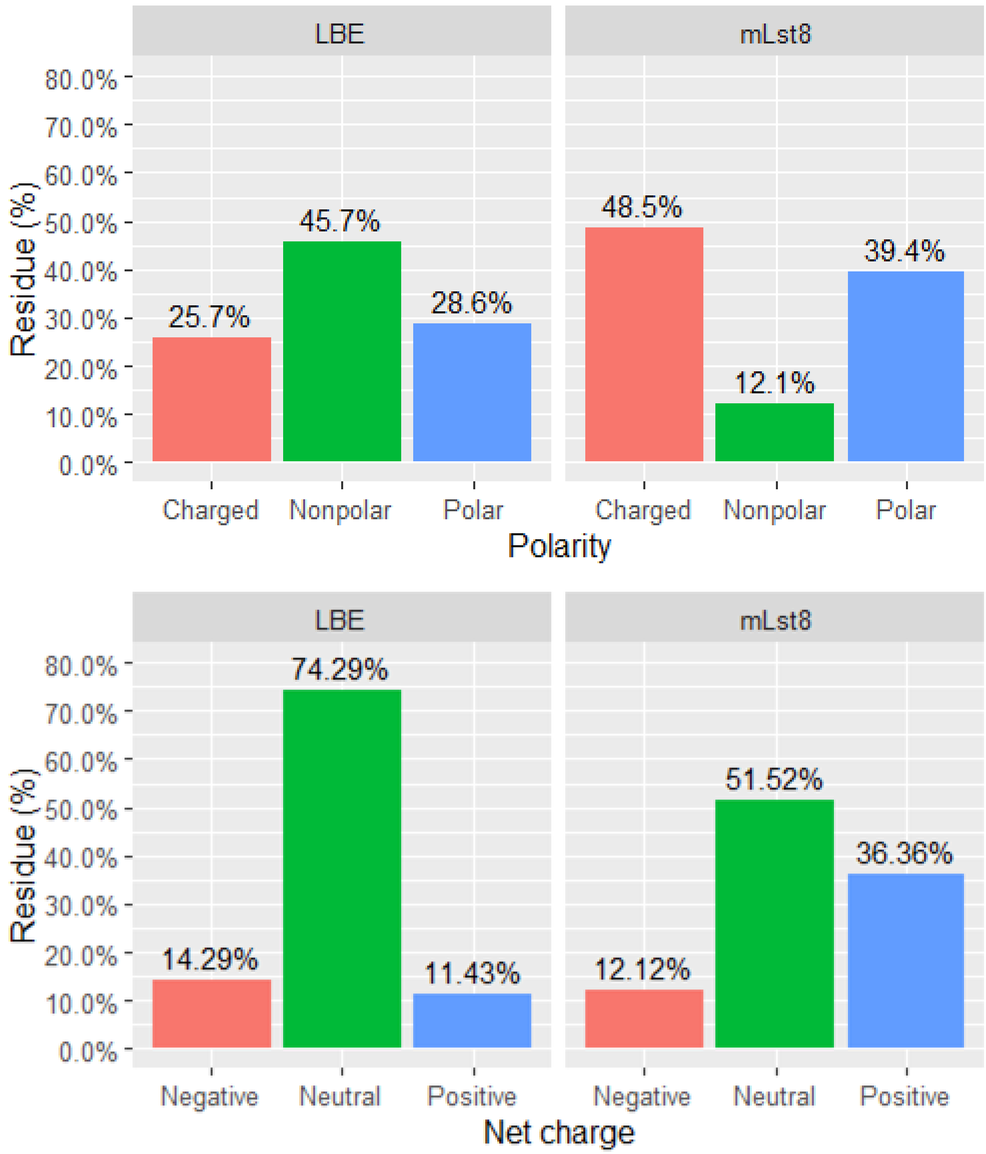

Figure 4. Amino acids characteristics from 68 residues of the LBE-mLst8 interface.

In the **Figure 5** are showed the boxplot and graphical representation of the main residues with negative energy values that contributed for FBE. 84.59% (-53.31 kcal/mol) of FBE is explained by through only 21 residues.

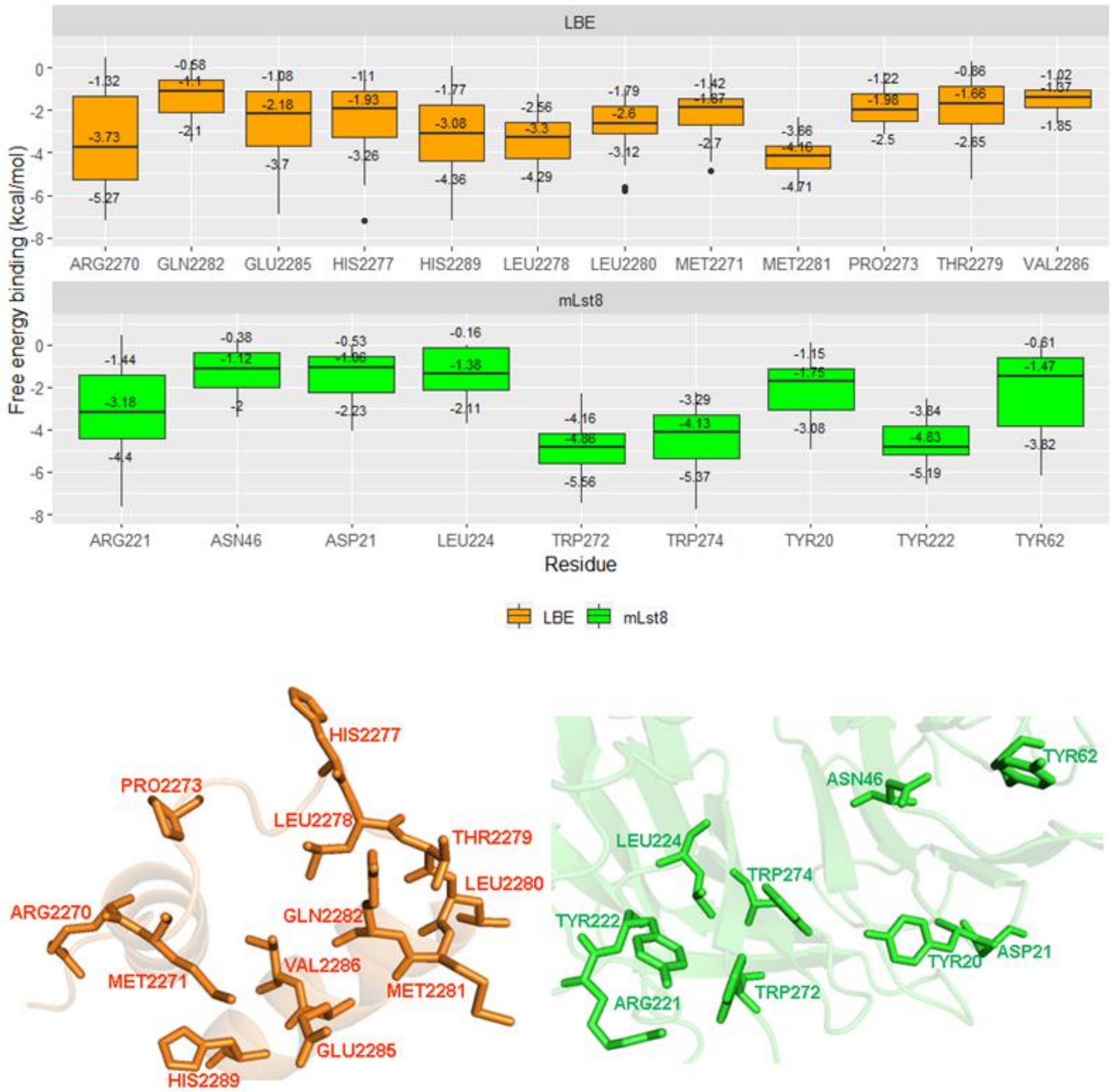

Figure 5. Box plot and graphical representation of the main residues that showed negative values of the FBE. The main residues are shown as sticks and the protein as cartoon.

Concerning the hydrogen bonds between LBE-mLst8 interface, we found 1436 interactions in the 51 evaluated systems. From these interactions, 2.1% are main chain–main chain (MM), 7,7% are main chain–side chain (MS), 35,9% are side chain–main chain (SM) and 54,4% are side chain–side chain (SS). The analysis of Donor–Acceptor (DA) distance revealed average 3.41 Å (SD ± 0.29 Å), median 3.46 Å (min 2.51 Å – max 3.80 Å). The Donor–Hydrogen–Acceptor (DHA) angle presented average 124.23° (SD ± 22.48°), median 121.18° (min 90.07° – max 179.22°). The Hydrogen–Acceptor (HA) distance average was 2.85 Å (SD ± 0.37 Å), median 2.87 Å (min 1.71 Å – max 3.67 Å).

Discussion

The proteins perform an important role in biological processes level and the PPIs are essential for triggering molecular mechanisms. However, the suppression or overexpression of specific pathways from these processes may lead to an organic disorder state and favoring the development of diseases. Currently, the major challenge is to understand how proteins can interact and what are the characteristics of these bindings to discover new potential PPIs modulators in therapeutic intervention. Concerning to reduce costs and time, the computational techniques are very useful to help the knowledge about PPIs because they may employ a crystallographic solved protein from a database, modeling structures, perform molecular dynamics simulations to evaluate the PPIs behavior and assess the results with statistical analysis to verify the method effectiveness and accuracy [5,58].

Over the last years, some therapeutic solutions were found based on PPIs. For example, the novel protein degradation technology called proteolysis targeting chimeric (PROTAC) is an effective endogenous protein degradation mechanism that can ubiquitinate the protein of interest (POI) through the ubiquitin-proteasome system (UPS) to reach an effect on a target. The main advantage of this target specificity aims to reduce the adverse effects like undesirable side effects, toxicity and low dose-response compared to conventional treatments, besides to reduce target resistance and to be a solution for undruggable targets. [26,27,59–62]. Currently, at least 15 PROTACs are under the firsts stages of clinical research and some of them already hits the clinic with satisfactory safety and efficacy profiles [63–68].

The first step to develop new drug strategies is understand the target behavior. In our case, we focused on evaluate the mTOR-mLst8 binding once that the kinase activation depends on the mLst8 binding [16,19]. Therefore, this feature by itself already demonstrates selectivity to the main target because there is not the kinase activation and subsequent pathway overexpression in diseases cases without mTOR-mLst8 binding.

Although the complex mTOR pathway is crucial for many biological processes, there is not many studies exploring mTOR-mLst8 interface in a molecular level. Thus, our study is the first to integrate coarse-grained molecular simulation, free-energy calculation, per-residue decomposition and hydrogen bonds identification to establish the mTOR-mLst8 binding profile and provide important knowledge to development of PROTACs heading to the mLst8 polyubiquitination because this affects indirectly the kinase activation and favor the degradation process of a small proteic portion as mLst8 (about 326 amino acids residues).

The first characterization of mTOR-mLst8 interaction was performed by Santos de Oliveira et al (2020) where the PPI calculations were performed at the quantum level, within the density functional theory (DFT) framework, to identify hotspots residues at the mTOR-mLst8 interface [69]. Althought a different method was employed, likewise, in our work we also suggest the relevance of mTOR residues ARG2270, HIS2289, LEU2278 and MET2281 and mLst8 residues ARG221, TRP272, TRP274 and TYR222 because they presented the lowest FBE values (median < 3.0 kcal/mol) and clearly these residues are directly involved in mTOR-mLst8 binding.

Furthermore Yang et al (2013) propose that the LBE-mLst8 interface involves mostly polar LBE residues and polar/aromatic mLST8 residues. However, in our study that explores only the residues that contribute for FBE, these residues are nonpolar/neutral for LBE and polar/neutral for mLst8 subunit. Possibly this difference may be related to use of the structures retrieved from the molecular dynamics each 1 ns (n = 1000) instead of only the crystallographic structure as shown by Yang et al [19].

Regarding the hydrogen bonds, we concluded that the majority of hydrogen bonds donors were related to ARG2270, LEU2278, LEU2280 and MET2281 from LBE fraction and ARG221, TRP272, TRP274, TYR20 and TYR222 from mLst8 subunit. For acceptors: ARG2270, MET2271 and MET2281 from LBE and ASP21, TYR20, TYR222 and TYR62 from mLst8. Whereas Yang et al (2013) also referred the mTOR-mLst8 interface is dominated by hydrogen bonds, they did not provide much information about these interactions [19].

Our findings are very relevant for future development of new strategies to control the important mTOR pathway because provide valuable information about this proteic interface. In fact, this study is the first to shown the residues' characteristics and the amount and types of hydrogen bonds involved in the proteins binding. Such information may be useful for the search of new PROTACs able to link the PROTAC warheads in the mLst8 binding interface and perform the degradation of mLst8 via proteassome.

Conclusion

In silico approaches can be very useful to elucidate biological mechanisms at molecular level. Employing a satisfactory sampling of the behavior of the mTOR-mLst8 complex through molecular simulation, we explored the mTOR-mLst8 interface using MM/GBSA approaches, free energy binding calculation and hydrogen bonds evaluation with statistical analysis. Our results reinforced the few previous mTOR-mLst8 studies and led to the identification of key amino acids and interactions contributing to the differential binding of mTOR-mLst8 and these findings could be applied to the development of new strategies to avoid the superexpression of this pathway.

Acknowledgements

We would like to acknowledge the team from Laboratorio de Simulaciones Biomoleculares of Institut Pasteur de Montevideo and Fernando Vieira Lazzarin.

Declarations

Funding: This research did not receive any specific grant from funding agencies in the public, commercial, or not-for-profit sectors.

Conflicts of interest/Competing interests: The authors declare that they have no conflict of interest.

Availability of data and material: N/A

Code availability: N/A

Authors' contributions: N/A

REFERENCES

[1] Salazar GA, Meintjes A, Mazandu GK, et al. A web-based protein interaction network visualizer. BMC Bioinformatics. 2014;15:129.

[2] Keskin O, Tuncbag N, Gursoy A. Predicting Protein–Protein Interactions from the Molecular to the Proteome Level. Chem Rev. 2016;116:4884–4909.

[3] Rao VS, Srinivas K, Sujini GN, et al. Protein-Protein Interaction Detection: Methods and Analysis. Int J Proteomics. 2014;2014:e147648.

[4] Klingström T, Plewczynski D. Protein–protein interaction and pathway databases, a graphical review. Brief Bioinform. 2011;12:702–713.

[5] Peng X, Wang J, Peng W, et al. Protein–protein interactions: detection, reliability assessment and applications. Brief Bioinform. 2016;bbw066.

[6] Saxton RA, Sabatini DM. mTOR Signaling in Growth, Metabolism, and Disease. Cell. 2017;168:960–976.

[7] Laplante M, Sabatini DM. mTOR signaling in growth control and disease. Cell. 2012;149:274–293.

[8] Laplante M, Sabatini DM. mTOR signaling at a glance. J Cell Sci. 2009;122:3589–3594.

[9] Boutouja F, Stiehm CM, Platta HW. mTOR: A Cellular Regulator Interface in Health and Disease. Cells [Internet]. 2019 [cited 2019 Sep 1];8. Available from: https://www.ncbi.nlm.nih.gov/pmc/articles/PMC6356367/.

[10] Hara K, Maruki Y, Long X, et al. Raptor, a binding partner of target of rapamycin (TOR), mediates TOR action. Cell. 2002;110:177–189.

[11] Fonseca BD, Smith EM, Lee VH, et al. PRAS40 is a target for mammalian target of rapamycin complex 1 and is required for signaling downstream of this complex. J Biol Chem. 2007;282:24514–24524.

[12] Sarbassov DD, Ali SM, Kim DH, et al. Rictor, a novel binding partner of mTOR, defines a rapamycin-insensitive and raptor-independent pathway that regulates the cytoskeleton. Curr Biol. 2004;14:1296–1302.

[13] Frias MA, Thoreen CC, Jaffe JD, et al. mSin1 is necessary for Akt/PKB phosphorylation, and its isoforms define three distinct mTORC2s. Curr Biol CB. 2006;16:1865–1870.

[14] Pearce LR, Huang X, Boudeau J, et al. Identification of Protor as a novel Rictor-binding component of mTOR complex-2. Biochem J. 2007;405:513–522.

[15] Kakumoto K, Ikeda J, Okada M, et al. mLST8 Promotes mTOR-Mediated Tumor Progression. PLoS ONE [Internet]. 2015 [cited 2019 Sep 1];10. Available from: https://www.ncbi.nlm.nih.gov/pmc/articles/PMC4408021/.

[16] Guertin DA, Stevens DM, Thoreen CC, et al. Ablation in mice of the mTORC components raptor, rictor, or mLST8 reveals that mTORC2 is required for signaling to Akt-FOXO and PKC alpha but not S6K1. Dev Cell. 2006;11.

[17] Kist R, Timmers LFSM, Caceres RA. Understanding the role of mTOR-mLst8 binding through coarse-grained simulation approaches. Mol Simul. 2021;47:1198–1207.

[18] Hua H, Kong Q, Zhang H, et al. Targeting mTOR for cancer therapy. J Hematol OncolJ Hematol Oncol. 2019;12:71.

[19] Yang H, Rudge DG, Koos JD, et al. mTOR kinase structure, mechanism and regulation. Nature. 2013;497:217–223.

[20] Yang H, Chen X, Liu M, et al. The structure of mTOR complexes at a glance. Precis Cancer Med. 2018;1:7–7.

[21] Neer EJ, Schmidt CJ, Nambudripad R, et al. The ancient regulatory-protein family of WD-repeat proteins. Nature. 1994;371:297–300.

[22] Dann SG, Selvaraj A, Thomas G. mTOR Complex1-S6K1 signaling: at the crossroads of obesity, diabetes and cancer. Trends Mol Med. 2007;13:252–259.

[23] Dazert E, Hall MN. mTOR signaling in disease. Curr Opin Cell Biol. 2011;23:744–755.

[24] Wang B, Jie Z, Joo D, et al. TRAF2 and OTUD7B govern a ubiquitin-dependent switch that regulates mTORC2 signalling. Nature. 2017;545:365–369.

[25] Deng L, Meng T, Chen L, et al. The role of ubiquitination in tumorigenesis and targeted drug discovery. Signal Transduct Target Ther. 2020;5:11.

[26] Pei H, Peng Y, Zhao Q, et al. Small molecule PROTACs: an emerging technology for targeted therapy in drug discovery. RSC Adv. 2019;9:16967–16976.

[27] Sun X, Gao H, Yang Y, et al. PROTACs: great opportunities for academia and industry. Signal Transduct Target Ther. 2019;4:1–33.

[28] Eswar N, Webb B, Marti-Renom MA, et al. Comparative protein structure modeling using Modeller. Curr Protoc Bioinforma. 2006;Chapter 5:Unit 5.6.

[29] Sali A, Blundell TL. Comparative Protein Modelling by Satisfaction of Spatial Restraints. 1993.

[30] Darré L, Machado MR, Brandner AF, et al. SIRAH: A Structurally Unbiased Coarse-Grained Force Field for Proteins with Aqueous Solvation and Long-Range Electrostatics. J Chem Theory Comput. 2015;11:723–739.

[31] Machado MR, Pantano S. SIRAH tools: mapping, backmapping and visualization of coarse-grained models. Bioinformatics. 2016;32:1568–1570.

[32] Darré L, Machado MR, Dans PD, et al. Another Coarse Grain Model for Aqueous Solvation: WAT FOUR? J Chem Theory Comput. 2010;6:3793–3807.

[33] Gonzalez HC, Darré L, Pantano S. Transferable Mixing of Atomistic and Coarse-Grained Water Models. J Phys Chem B. 2013;117:14438–14448.

[34] Caceres-Delpiano J, Wang L-P, Essex JW. The Automated Optimisation of a Coarse-Grained Force Field Using Free Energy Data [Internet]. Biophysics; 2020 [cited 2021 May 9]. Available from: http://biorxiv.org/lookup/doi/10.1101/2020.08.13.250233.

[35] Darré L, Tek A, Baaden M, et al. Mixing Atomistic and Coarse Grain Solvation Models for MD Simulations: Let WT4 Handle the Bulk. J Chem Theory Comput. 2012;8:3880–3894.

[36] Dolinsky TJ, Nielsen JE, McCammon JA, et al. PDB2PQR: an automated pipeline for the setup of Poisson-Boltzmann electrostatics calculations. Nucleic Acids Res. 2004;32:W665-667.

[37] Abraham MJ, Murtola T, Schulz R, et al. Gromacs: High performance molecular simulations through multi-level parallelism from laptops to supercomputers. SoftwareX. 2015;1–2.

[38] Van Der Spoel D, Lindahl E, Hess B, et al. GROMACS: fast, flexible, and free. J Comput Chem. 2005;26:1701–1718.

[39] Darden T, York D, Pedersen L. Particle mesh Ewald: An N· log (N) method for Ewald sums in large systems. J Chem Phys. 1993;98:10089–10092.

[40] Bussi G, Donadio D, Parrinello M. Canonical sampling through velocity rescaling. J Chem Phys. 2007;126:014101.

[41] Parrinello M, Rahman A. Polymorphic transitions in single crystals: A new molecular dynamics method. J Appl Phys. 1981;52:7182–7190.

[42] Kagami LP, das Neves GM, Timmers LFSM, et al. Geo-Measures: A PyMOL plugin for protein structure ensembles analysis. Comput Biol Chem. 2020;87:107322.

[43] Van Rossum G, Drake Jr. FL. Python reference manual. Amsterdam: Centrum voor Wiskunde en Informatica.; 1995.

[44] Weng G, Wang E, Wang Z, et al. HawkDock: a web server to predict and analyze the protein–protein complex based on computational docking and MM/GBSA. Nucleic Acids Res. 2019;47:W322–W330.

[45] Gurusaran M, Sivaranjan P, Dinesh Kumar KS, et al. Hydrogen Bonds Computing Server (HBCS): an online web server to compute hydrogen-bond interactions and their precision. J Appl Crystallogr. 2016;49:642–645.

[46] Word JM, Lovell SC, Richardson JS, et al. Asparagine and glutamine: using hydrogen atom contacts in the choice of side-chain amide orientation 1 1Edited by J. Thornton. J Mol Biol. 1999;285:1735–1747.

[47] Fisher SJ, Wilkinson J, Henchman RH, et al. An evaluation review of the prediction of protonation states in proteins *versus* crystallographic experiment†. Crystallogr Rev. 2009;15:231–259.

[48] Team RC. R: A language and environment for statistical computing. R Foundation for Statistical Computing, Vienna, Austria.[WWW document]. URL Httpwww R-Proj OrgAccessed Dec 24 2013. 2013;

[49] Shapiro SS, Wilk MB. An analysis of variance test for normality (complete samples). Biometrika. 1965;52:591–611.

[50] Spearman C. The Proof and Measurement of Association between Two Things. Am J Psychol. 1904;15:72.

[51] Ramachandran KM, Tsokos CP. Nonparametric Statistics. Math Stat Appl R [Internet]. Elsevier; 2021 [cited 2021 Oct 23]. p. 491–530. Available from: https://linkinghub.elsevier.com/retrieve/pii/B9780128178157000129.

[52] Friedman M. The Use of Ranks to Avoid the Assumption of Normality Implicit in the Analysis of Variance. J Am Stat Assoc. 1937;32:675–701.

[53] Friedman M. A Correction: The Use of Ranks to Avoid the Assumption of Normality Implicit in the Analysis of Variance. J Am Stat Assoc. 1939;34:109.

[54] Friedman M. A Comparison of Alternative Tests of Significance for the Problem of m Rankings. Ann Math Stat. 1940;11:86–92.

[55] Nemenyi PB. Distribution-free multiple comparisons. Princeton University; 1963.

[56] Kastritis PL, Rodrigues JPGLM, Folkers GE, et al. Proteins Feel More Than They See: Fine-Tuning of Binding Affinity by Properties of the Non-Interacting Surface. J Mol Biol. 2014;426:2632–2652.

[57] Cooper GM, Hausman RE, Hausman RE. The cell: a molecular approach. ASM press Washington, DC; 2007.

[58] Cicaloni V, Trezza A, Pettini F, et al. Applications of in Silico Methods for Design and Development of Drugs Targeting Protein-Protein Interactions. Curr Top Med Chem. 2019;19:534–554.

[59] He Y, Khan S, Huo Z, et al. Proteolysis targeting chimeras (PROTACs) are emerging therapeutics for hematologic malignancies. J Hematol OncolJ Hematol Oncol. 2020;13:103.

[60] Qi S-M, Dong J, Xu Z-Y, et al. PROTAC: An Effective Targeted Protein Degradation Strategy for Cancer Therapy. Front Pharmacol. 2021;12:1124.

[61] Gao H, Sun X, Rao Y. PROTAC Technology: Opportunities and Challenges. ACS Med Chem Lett. 2020;11:237–240.

[62] Pettersson M, Crews C. PROteolysis TArgeting Chimeras (PROTACs) - Past, Present and Future. Drug Discov Today Technol. 2019;31:15–27.

[63] Mullard A. First targeted protein degrader hits the clinic. Nat Rev Drug Discov. 2019;18:237–239.

[64] Mullard A. Targeted protein degraders crowd into the clinic. Nat Rev Drug Discov. 2021;20:247–250.

[65] Mullard A. Targeted degraders clear first safety hurdles. Nat Rev Drug Discov. 2020;19:435.

[66] Petrylak DP, Gao X, Vogelzang NJ, et al. First-in-human phase I study of ARV-110, an androgen receptor (AR) PROTAC degrader in patients (pts) with metastatic castrate-resistant prostate cancer (mCRPC) following enzalutamide (ENZ) and/or abiraterone (ABI). J Clin Oncol. 2020;38:3500–3500.

[67] Ambrosini M, Fucà G, Duca M, et al. Targeted protein degraders from an oncologist point of view: The Holy Grail of cancer therapy? Crit Rev Oncol Hematol. 2022;169:103532.

[68] Flanagan J, Qian Y, Gough S, et al. Abstract P5-04-18: ARV-471, an oral estrogen receptor PROTAC degrader for breast cancer. 2019;

[69] Santos de Oliveira FL, Vieira Carletti J, Azevedo FFN, et al. mTOR–mLST8 interaction: hot spot identification through quantum biochemistry calculations. New J Chem. 2020;44:20982–20992.

4 CONCLUSÃO

As técnicas computacionais são essenciais para adquirir conhecimento sobre o comportamento de vias de sinalização compostas por biomoléculas. No presente trabalho apresentamos um passo inicial para o desenvolvimento de estratégias de controle da via da mTOR. Ao final, conseguimos elucidar alguns pontos importantes relacionados ao comportamento da quinase frente ao acoplamento da subunidade mLst8 à quinase mTOR e reforçar estudos prévios de que esse acoplamento é necessário para ativação e ação fosforilativa. Além disso, conseguimos detalhar a interface de acoplamento mLst8-mTOR a fim de possibilitar estudos futuros relacionados à novas estratégias de controle da via de sinalização como, por exemplo, desenvolvimento de PROTACs capazes de encaminhar a subunidade mLst8 para degradação via proteassoma e evitar a superexpressão e descontrole fisiopatológico da via de sinalização.

Do ponto de vista experimental, podemos implementar técnicas capazes de validar nossos métodos apresentados como, por exemplo, a Espectrometria de Massa de Troca de Hidrogênio/Deutério (HDX-MS) que visa analisar características estruturais (interações proteína-proteína e volume cavitário do sítio catalítico) sendo capaz de fornecer informações sobre proteínas individuais, bem como grandes complexos proteicos (OZOHANICS; AMBRUS, 2020). De mesma forma, para se avaliar a capacidade fosforilativa da mTOR quando a fração mLst8 está associada ou não, podemos dispor de métodos cinéticos enzimáticos (ADMIRAAL; HERSCHLAG, 1995; HERSCHLAG; JENCKS, 1990; MATTE; TARI; DELBAERE, 1998).

5 PERSPECTIVAS

Mesmo após mais de 8 anos de pesquisas dedicadas a via de sinalização da mTOR ela sempre parece a fornecer detalhes interessantes, a cada trabalho realizado mais resultados são obtidos e novas hipóteses são propostas. Nos estudos prévios, utilizamos o mecanismo inibitório para sugerir novos potenciais inibidores da quinase e então, compreendendo o processo de ativação da via metabólica, ficou evidente que o controle de ativação da quinase pode ser valioso visto que é comum aos dois complexos existente nos organismos biológicos e pode ser uma via específica de controle.

Dessa forma, os próximos passos são utilizar os dados prévios obtidos neste trabalho para avaliar a potencialidade do emprego da tecnologia de PROTACs no controle da via metabólica, lançando o desafio de realizar estudos de docagem e simulação do complexo mTOR-mLst8 para este fim.

6 ANEXOS

6.1 Carta de aceite do Artigo I (DOI 10.1080/08927022.2021.1962525)

Gmail

Roger Kist <rogerkist@gmail.com>

Taylor & Francis author update: access to your article published in an issue of Molecular Simulation

1 mensagem

Taylor & Francis <noreply@tandfonline.com> 18 de agosto de 2021 01:56
Responder a: support@tandfonline.com
Para: rogerkist@gmail.com

Taylor & Francis Online

The online platform for Taylor & Francis Group content

Author Services | FAQ | Twitter | Facebook | LinkedIn

Dear Roger Kist,

Your article, Understanding the role of mTOR-mLst8 binding through coarse-grained simulation approaches, published in Molecular Simulation, Volume 47 Issue 14, is now available for you to access via tandfonline.com.

You will have permanent, free access to the final published version of your article via your Authored Works, our dedicated center for all Taylor & Francis authors. This is where you can view all articles published in our journals, check how many people have viewed them, see their citations, and check your Altmetric data. Haven't registered for your Authored Works yet? Find out how.

6.2 Carta de submissão do Artigo II

Gmail Roger Kist <rogerkist@gmail.com>

Journal of Biomolecular Structure & Dynamics - Manuscript ID TBSD-2021-2302 has been submitted online

1 mensagem

Journal of Biomolecular Structure & Dynamics <onbehalfof@manuscriptcentral.com> 30 de dezembro de 2021 22:32

Responder a: TBSD-peerreview@journals.tandf.co.uk
Para: rogerkist@gmail.com

30-Dec-2021

Dear Mr Kist:

Your manuscript entitled "The mTOR-mLst8 binding profile through molecular simulation, free-energy calculation, per-residue decomposition and hydrogen bonds identification" has been successfully submitted online and is presently being given full consideration for publication in Journal of Biomolecular Structure & Dynamics.

Your manuscript ID is TBSD-2021-2302.

Please mention the above manuscript ID in all future correspondence or when calling the office for questions. If there are any changes in your street address or e-mail address, please log in to ScholarOne Manuscripts at https://mc.manuscriptcentral.com/jbsd and edit your user information as appropriate.

You can also view the status of your manuscript at any time by checking your Author Center after logging in to https://mc.manuscriptcentral.com/jbsd.

If you do not hear from the editor within 2 months, please contact me.

Thank you for submitting your manuscript to Journal of Biomolecular Structure & Dynamics.

Sincerely,
Journal of Biomolecular Structure & Dynamics Editorial Office